hybrid GEOTABS

Controlling the power of the ground by integration

# D2.5

# hybridGEOTABS key component sizing methodology and guidelines

Author: **UGent**

Date: **February 2021 (M54)**

Version: 1.0

Dissemination level: Public

Funded by the European Commission under the Horizon 2020 Programme: project number 723649 (proposal name "MPC-;GT")

Controlling the power of the ground by integration

**Original title:** Specifications of a set of standardised modular hybridGEOTABS component packages

**Lead beneficiary:** BOY (Boydens Engineering, Belgium)

**Deliverable lead:** UGent (Ghent University, Belgium)

**Author(s):** UGent (Ghent University, Belgium)

Mohsen Sharifi (mohsen.sharifi@ugent.be)

Rana Mahmoud

Josué Borrajo Bastero

Eline Himpe (eline.himpe@ugent.be)

Jelle Laverge

**Reviewer(s):** Viessmann (Belgium)

Jan Hoogmartens

**Deliverable history:** Version 1.0: February 2021 (M54)

**Dissemination level:** Public

## Summary

During the early design stages, namely feasibility study and pre-design, the HVAC-designer proposes one or several suitable HVAC-solutions for a building project. Often, the project is not yet contracted at that point (for example in context of design competitions) and therefore the HVAC-designer is severely limited in the amount of resources that can be allocated. Additionally, the architectural design is still very much in flux at this point and will only be specified in more detail at a later stage. The designer therefore needs to be able to provide the client with feedback about the implications of high level design choices, such as broad volumetric choices, overall thermal performance of the envelope or window-to-wall ratio, on the choice of the HVAC system. For conventional systems there are straightforward and cheap methodologies that are commonly used. However, in a competitive market with increasing energy-efficiency objectives, and more complex buildings and HVAC, the simplified methods are not satisfactory anymore. This applies to buildings with hybrid systems, especially with integrated renewables, and to buildings where thermal storage and thermal inertia play an important role. In other words, in many buildings, such as hybridGEOTABS, that do fit in the energy-efficiency objectives and energy system designs in a transition to a low-carbon society [1]. Simplified design methods (such as steady-state standardized calculations) do not account for an optimal sizing of hybrid systems, or for the effects of thermal inertia in the building and/or system, leading to either an inaccurate and often oversized system with high investment costs, or very expensive and complicated design procedures, both leading to higher costs and lower chances to realise these environmentally friendly and efficient solutions. Here is where the trade-off between accuracy and investment becomes clear.

Nonetheless, the hybridGEOTABS design is worthy of and accurate sizing methodology/tool since the investment cost could be remarkably decreased by appropriately sizing the components. On the other hand, achieving the optimal sizing is neither an easy task for every designer nor cheap for the customer in terms of engineering costs. Therefore, the number of GEOTABS project are limited to the narrow range of the buildings which are appropriate for GEOTABS and limited number of companies which have been practicing the design formerly. Here is the need for an easy and fast and optimal sizing methodology for hybridGEOTABS component to spread their usage in order to increase the renewable sources share in buildings.

Having a high thermal inertia, Thermally Activated Building Systems (TABS) can provide the thermal comfort with a low-exergy source such as a ground source heat pump. However, TABS is different from many other emission systems since it is using conduction heat transfer inside the TABS and radiation and convection at the surface to the room. The conduction heat transfer throughout the concrete layers of a TABS-floor results in a delay between the heat that is injected to the TABS and the heat that is received in the room. Additionally, the radiation heat transfer is a function of the two sides temperature difference, room temperature and TABS surface temperature. Conclusively, dynamic simulation is an evitable part of the design when TABS is used. Moreover, the power of TABS is very sensitive to the control system and the temperature of the two sides. For instance in heating mode with a smart control, it is possible to store energy in the TABS during day and release it during night (peak shaving). Similarly, TABS has a self-regulating effect meaning that when the load in the room increases, the temperature difference between TABS and the room increases and thus surface temperature tends to become closer to the room temperature and as a result the power of TABS also increases automatically. These features and others are important benefits of TABS and must be incorporated in the design.

An accurate algorithm with consideration of the aforementioned phenomena is explained in D2.3 and D2.4, where the optimal control is integrated into the rather detailed dynamic simulations and an optimal HVAC-sizing is found with an optimization algorithm. The exercise in D2.4 reveals the high potential of the optimal design for hybridGEOTABS, leading to a significant optimization of the investment (and operation) costs of the system as indicated by the net present value. However, the algorithm explained in D2.4 is computationally intensive and, today, still requires experts to perform.

Therefore, a more straightforward-to-use and fast methodology is developed in WP2. The methodology is based on a database of pre-simulated, multizone dynamic heating and cooling demand curves for a large variety of office buildings, schools, elderly homes and multi-family residential building typologies throughout the EU, with varying building geometrical and building physical properties, as documented in D2.2 [7, 2]. The accompanying load splitting algorithm emulates the behaviour of an optimal controller to split the load between the TABS and a secondary emission system while respecting thermal comfort and accounting for the TABS thermal properties, as documented in D2.1. Then, as documented in the underlying deliverable D2.5 , the outputs of the load splitting algorithm as applied to the building stock cases, are post-processed to come up with the final sizing and performance estimate of the hybridGEOTABS system components. The process is applied to the building stock cases and design guidelines are provided under the shape of design decision trees.

In this report, the steps and assumptions which are needed to go from the time series split to the final sizing and performance estimation are elaborated (chapter 2). First, the estimation of the geothermal heat pump size, based on smoothing of the baseload time series, is explained and validated. In a second post-processing step the thermal balance of the borefield is implemented based on the assumption that the heat injected to the borefield accounts for 40% to 60% of the total heat exchanged between the borefield and the building ("the 40-60 rule"). A complete overview of this calculation-efficient hybridGEOTABS sizing and performance estimation process is incorporated in section 2.6. The procedure is then applied to the 5 case-study buildings used in D2.4, and the outcomes are compared to the outcomes provided by a detailed, but more calculation-intensive, optimal sizing algorithm developed in T2.3 of the project (chapter 3). It is concluded that the results of the hybridGEOTABS sizing process are in the same order of magnitude, or a bit on the 'safe side' (higher), which is a welcome result in context of a pre-design study. In general, the outcomes of both design methods lead to a clearly smaller sizing than traditional steady-state design calculations. Secondly, the results indicate that the borefield balancing using the "40-60 rule" should be understood as "cautious" results, while higher imbalances between injected and extracted heat in the borefield may not harm the long-term performance of the borefield. Therefore, the results of the sizing process can be understood as a 'minimum' feasible share of GEOTABS, restricted by the thermal borefield balance, while from the perspective of the TABS only shares higher than 75% are feasible for the majority of building cases, representing the further optimisation potential in a more detailed borefield design and/or consideration of borefield regeneration options.

Finally, the hybridGEOTABS sizing and performance estimation process is applied to over 140,000 case-study buildings using an automated software code (chapter 4). The results provide a rich database as a basis for the hybridGEOTABS design webtool (D2.6). In the current report, meta-analysis of the data is carried out to come up with design guidelines for the key components of hybridGEOTABS (chapter 5). The main outcome of the whole procedure is a set of four design decision trees providing the most crucial inputs for the designer to consider in the early design stage, and the key sizing and performance indicators. The decision trees are provided for four different typologies attached to this report, and are available on the hybridGEOTABS website. While using the decision tree for design is very fast and easy, the results are close to the results coming from detailed and time consuming algorithms, and are thus an added value for the designer to assess the feasibility of hybridGEOTABS for their design. Moreover, architects can see the influence of different parameters on the sizing and performance of the system. Thus, they may use it to optimise the building physical design to increase the possible share of GEOTABS as a sustainable core for providing thermal comfort in buildings.

# Table of Contents

## Contents

# Nomenclature

## Acronyms

| | |
|---|---|
| BES | Building Energy Simulation |
| COP | Coefficient of Performance |
| $CO_2$ | Carbon Dioxide |
| FCU | Fan Coil Unit |
| GEOTABS | system combining TABS and geothermal energy using a heat pump |
| GSHP | Ground Source Heat Pump |
| GSHX | Ground Source Heat Exchanger |
| HP | Heat Pump |
| HVAC | Heating, Ventilation and Air Conditioning |
| MPC | Model Predictive Control |
| PCM | Phase-change materials |
| PV | Photovoltaic |
| RBC | Rule-based Control |
| RES | Renewable energy sources |
| $R^2ES$ | Renewable and residual energy sources |
| TABS | Thermally Active Building System |

# 1. hybridGEOTABS design challenges and solutions

## 1.1. hybridGEOTABS components

GEOTABS is an acronym for a geothermal heat pump (GEO), as energy supplier, combined with a Thermally Activated Building System (TABS) as emission system. One of the main challenges of GEOTABS especially in buildings with fast changing heating and cooling needs is to compensate sudden or fast changes. The main result is that the application of the concept has been limited to a relatively narrow range of 'suitable' building types, mostly office buildings with appropriate thermal insulation, modest internal gains and window-to-wall ratios. The recent developments in MPC allow for the extension of the application of the GEOTABS concept to a broader range of building types, since the load and discharge cycles of the TABS can be better scheduled to fit the anticipated fluctuations in the heating and cooling demand. The range of application is, however, still limited by the physical properties of the TABS and the building envelope.

By introducing a fast reacting secondary emission system, the hybridGEOTABS concept extends the applicability of GEOTABS to the point that it can be claimed that "*every building deserves a share of GEOTABS*". Within the constraints of the system properties, an as large as possible share of the heating and cooling loads are covered by the GEOTABS system, while the secondary system covers the remaining peak loads and fast fluctuations. This changes the main question facing the designer and his/her client during the design process from "*should we consider GEOTABS for this project?*" to "*what combination of GEOTABS and other system components is the most appropriate for this project?*". The hybridGEOTABS concept thus becomes the design strategy. To start with the design procedure of hybridGEOTABS, the key components of the concept have to be pointed out. For the beginning, a simplified schematic of the system is introduced in Figure 1-1. The key components are the heat pump (HP), ground source heat exchanger (GSHX), secondary production system in heating (e.g boiler), secondary production system in cooling (e.g. chiller), primary emission system (TABS), secondary emission system (e.g. FCU). Therefore, we aim to provide an easy guide for the designers to calculate the aforementioned components easily and optimally with logical assumptions and simplifications.

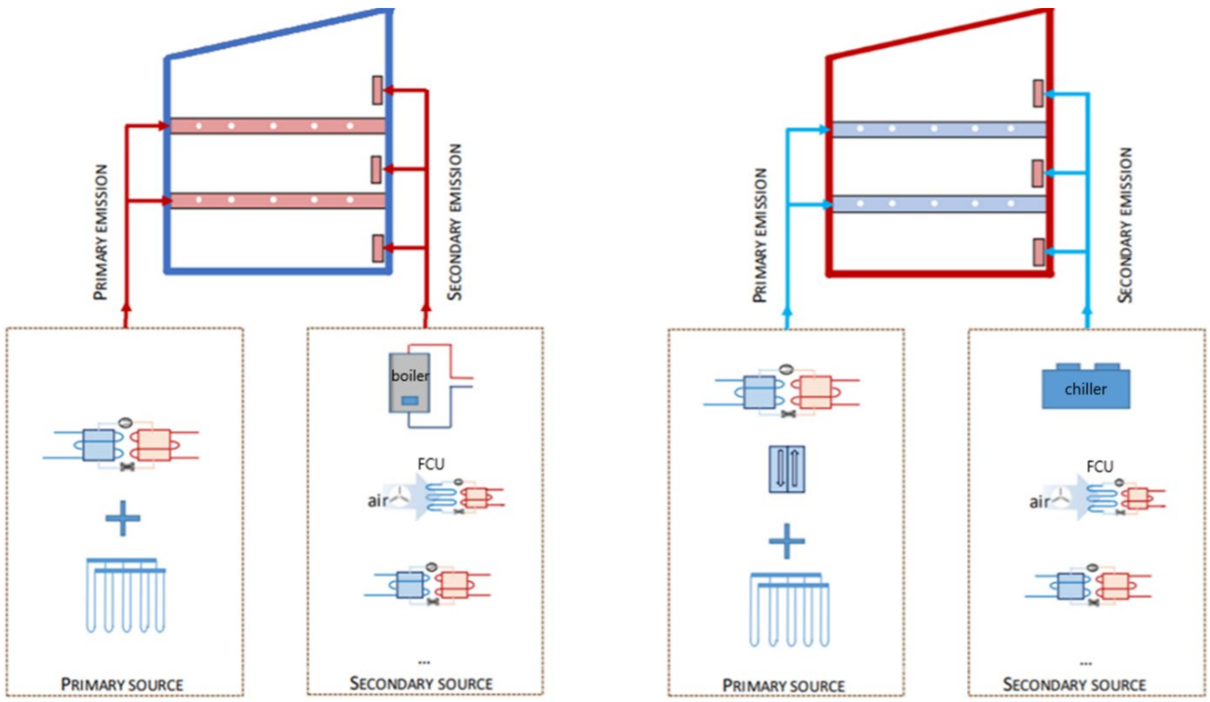


*Figure 1-1 schematic of hybridGEOTABS components in heating (left) and cooling (right)*

## 1.2. Design challenges

The design of hybrid and storage-integrated systems such as hybridGEOTABS, brings along challenges when it comes to the HVAC-design. The main questions are what shares of the heating and cooling demands can be optimally covered by the GEOTABS and secondary system respectively, and what are the resulting sizes of the key HVAC-components (the heat pump, geothermal borefield and secondary system). As a result of their thermal inertia, and if well-controlled, the heat inputs to the TABS can be smoothed out over time, resulting in peak shaving and reduced size of the heat pump. On the other hand, as it takes some time to charge and discharge this thermal storage, a sudden change from heating to cooling mode of the system would lead to energy losses. Therefore in such situations, it is often more desirable to engage a secondary fast-reacting emission system (e.g. fan coil units, air handling systems...). Yet another element to consider is the effect of the MPC on the component sizing and load shares. MPC optimises the system performance, and has knowledge of the building and system properties and behaviour (by using a model) and of future disturbances (by using predictions, e.g. weather predictions). This allows the controller to anticipate future demands, and thus reduce the peak powers that would otherwise be needed to maintain thermal comfort.

The aforementioned dynamic aspects influence the sizing and load share of the hybridGEOTABS system. As a result, the critical conditions for the sizing of the system(s), typically appearing at the warmest and coldest days of the year, are no longer valid for hybridGEOTABS buildings, and will lead to an oversizing of the system and increased investment costs. The steady-state heat loss calculation methods that are traditionally used to estimate the peak loads on the warmest and coldest day(s) of the year may therefore not result in the most critical load conditions for each of the hybridGEOTABS component. Moreover they do not allow to estimate the dynamic evolutions of the energy demands throughout the seasons, nor to split the loads and energy supply shares between the two systems. Instead, the state-of-the-art design of GEOTABS buildings today relies on detailed, case-by-case dynamic building energy simulations (BES), performed by experts. Especially in the early design stages, where budgets are often limited, and where even the basic design properties may still vary considerably, this is a significant barrier for considering hybridGEOTABS solutions. Therefore, there is a need for more straightforward and easy-to-use design tools to assist the designer in assessing the sizing and performance of the system in the early design stage, that however do take into consideration the dynamic aspects of the building, the systems and control.

## 1.3. Design solutions

The increasing availability of computational power, of the possibilities of BES-programs and of the storage of and access to large amounts of data, open new opportunities to tackle the aforementioned design challenge in a different way. By **pre-simulation and pre-engineering of the hybridGEOTABS pre-design for a large variety of buildings**, the complex and time-consuming efforts of the individual design engineer in the early design stage are reduced to the search for the available case-study building that approaches best his/her project, and the study of the resulting design solutions for varying building design properties. At the same time, it allows a dedicated research study and implementation of the aforementioned dynamic aspects influencing the design. This results in an interesting trade-off between effort and quality for designers in the early building and HVAC-design stages. The resulting database is made available via a web-tool (D2.6). Moreover, the meta-analysis of the database inputs and outputs allows to set up general guidelines for key component sizing and energy and environmental performance. The underlying report provides an overview of this pre-simulation and pre-engineering methodology (chapter 2) and verification against a detailed optimal control-integrated sizing algorithm (chapter 3). After application of the design process to all building stock cases, a meta-data analysis gave lead to the classification of buildings into groups with similar properties, translated into design decision trees for the HVAC-designer / architect and as a basis for the creation of key component packages (chapter 4 and 5).

# 2. hybridGEOTABS sizing and performance estimation process

## 2.1. Building thermal loads time series

The first step for sizing the components of an HVAC system is to estimate the building heating and cooling (peak) loads. There are numerous tools for load estimation. In general, the load can be calculated either statically according to the existing standards[1] or dynamically with building energy simulation (BES)-tools. In order to take into account the dynamic behaviour of the building, HVAC-system and control of hybridGEOTABS buildings, the use of dynamic BES is recommended. As the set-up of these simulations may be too time-consuming during the early design stages, a first step in the hybridGEOTABS design methodology is the pre-simulation of the hourly heating and cooling demands during one year using dynamic BES-models for a variety of buildings in the building stock. These simulations are made for about 140.000 buildings including four building typologies (offices, schools, elderly homes and multi-family buildings) and 3 different climatic zones in Europe.

In order to realise this high amount of simulations within a reasonable time-frame, the focus is on a rather detailed multi-zone model of the building, modelling of the occupancy and gains, the solar shading and ventilation strategy, which are influencing the heating and cooling demands. To maintain comfort in the building an ideal heating and cooling system is assumed in these simulations, that maintains the indoor temperature. The actual GEOTABS and secondary system components, as well as the control, are not included in these BES-models. Their behaviour are incorporated in subsequent steps.

The pre-simulation of the building stock cases is documented in detail in D2.2 and Mahmoud et al. 2.19 [7]. An overview of the properties of the simulated cases from the building stock is also available in D2.6. The times series are used as the input for further analysis explained in the next step.

## 2.2. Load splitting using the baseload algorithm

After calculating the building heating and cooling load time series, we can start with the sizing procedure. Sizing the key components of hybridGEOTABS starts with splitting the load between the primary and the secondary systems. In Task 2.1 of the project, a *baseload algorithm* was developed and validated for such splitting using the building thermal load time series derived in T2.2 (see section 2.1). The baseload is defined as the maximum share of GEOTABS that allows to minimise the energy use of the entire (primary + secondary) heating and cooling system, while maintaining thermal comfort in the building and by using and taking into account the thermal storage in the TABS. The baseload algorithm is the mathematical formulation of the baseload definition. The algorithm minimises the total energy use for heating and cooling of a building for an entire year, using the building heating and cooling demand as an input, and the thermal comfort and thermal inertia of the TABS as constraints. The outputs of the optimisation problem are the baseload and residual load and thus the shares of the primary GEOTABS system and the secondary system, as for example in Figure 2-1. Thus the outcome of the baseload algorithm for each case is time series of the primary and secondary system load for the entire year. These outputs are the basis for sizing the hybridGEOTABS key components via a subsequent post-processing step, that is documented in this deliverable. The baseload algorithm is documented in detail in D2.1 and Sharifi et al. 2019a and Sharifi et al. 2019b [4, 5].

---

[1] For example ISO 13790:2008 and EN 12831-1:2017

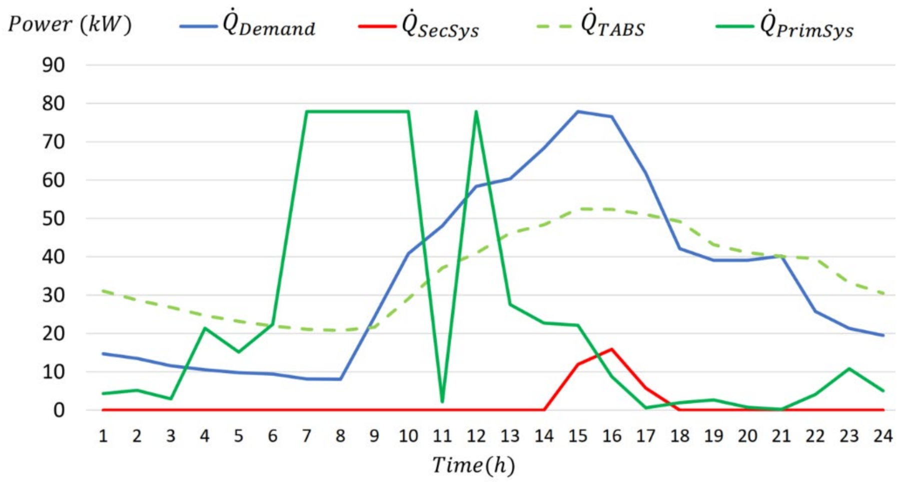


*Figure 2-1 Baseload algorithm outputs for one day of simulation, times series of the building heating and cooling demand, primary system power, Power of TABS in the room side, the secondary system power*

## 2.3. From load splitting to sizing: primary system size

As seen in Figure 2-1 the primary system power is constrained to a maximum, and this maximum is often reached for short periods of time after which the power drops significantly. This behaviour, which almost reminds of an on/off behaviour between very high and low powers, is observed throughout the year and throughout the cases (see D2.1). Here we shorty explain the reasons and consequences of this behaviour. Then, we explain how to deal with outcomes of the baseload algorithm to obtain final sizing of the components. The reasons for this behaviour are some features regarding the TABS and regarding the heuristic optimisation algorithm that is used in the baseload algorithm.

Regarding the heuristic optimization algorithm, the baseload algorithm is using a constrained optimisation algorithm when the system is linear. This speeds up the calculation time of the algorithm, but also means that the optimal solutions found by the algorithm are mostly close to the boundaries of the feasible domain for the primary system since the response time for this system is high. As a matter of fact, the borders of the solution space are the optimisation constraints which are chosen deliberately as maximum heating and cooling demands of the building. Therefore, the maximum load for the primary system (as an outcome of the baseload algorithm) appears to be equal to the maximum heating and cooling demands of the building.

On the other hand, regarding the TABS, the high thermal storage capacity and inertia of TABS provide some flexibility as to when the TABS is charged by the GSHP. This time shift between charging of the TABS and releasing the heat to the building zones, also allows to spread the charging over a longer period of time and thus shave the peak powers of the GSHP. Such feature thus can lead to downsizing of the heat pump. This advantage could automatically be captured by an optimisation algorithm, for example by including the HVAC investment cost in the cost function so the algorithm (that seeks to minimize the cost) sees advantages to start charging sooner and to decrease the primary system peak power. However, including this feature into the optimisation algorithm would explode its calculation time. Therefore, as an alternative, it was decided to mimic this behaviour in a post-processing of the baseload algorithm outcomes. Remark that for the secondary system none of the aforementioned issues appear because it is fairly assumed that there is no delay between the heat injected to the emission system and the heat received by the room, leaving no flexibility to the algorithm into when the heat is injected.

Sourbron [6] carried out a frequency analysis revealing an important feature of TABS from the control point of view. It shows that the system reaction to the control signals with high frequencies is relatively small. Therefore, the controller should instead control TABS with low frequency signals. Figure 2-2 shows that hourly changes of the heat injected are barley captured by TABS (especially when less than 10 hours). TABS needs more time to transfer heat form the pipes to the room side. Although Sourbron [6] is assuming a constant temperature in the room side to provide an analytic solution for the conductive heat transfer in the concrete of TABS, the heat demand in the building side is periodic and is effective on the heat transfer rate. Fast Fourier transform of the building heating and cooling demands shows that the most dominant periodicity of the building demand is 24 hours, which is the daily cycle of the weather conditions and of human behaviour. Conclusively, TABS can efficiently overcome the dominant frequent heating and cooling demand even with a smooth control signal. Consequently, the time series of the primary system derived from the baseload algorithm are smoothed to avoid having high peaks for the primary system and prevent oversizing of the system. Smoothing the primary system time series might be a double-edged-sword and therefore the consequences are carefully investigated in the next section.

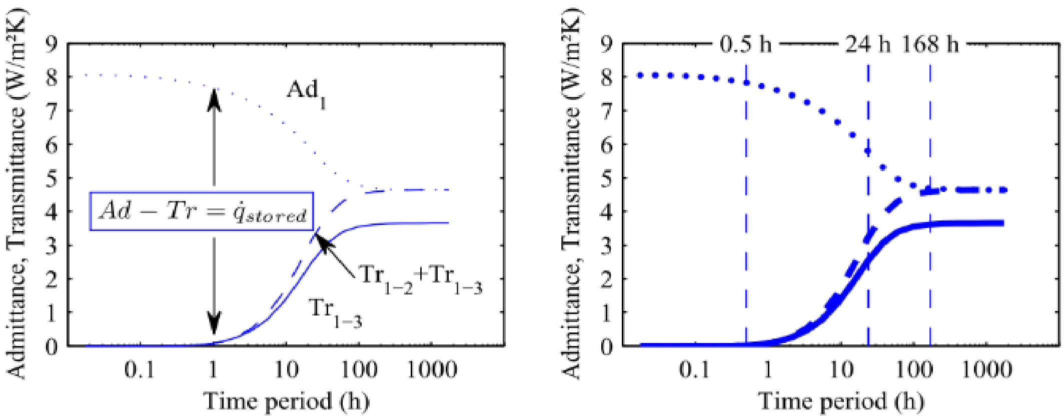


*Figure 2-2 Admittance, transmittance and stored energy in TABS in terms of time [6]*

### Post processing method (Smoothing with moving average)

Figure 2-3 shows an example of a one year primary system load time series as an outcome of the baseload algorithm (in grey), showing a lot of fluctuations, as explained before. Smoothed signals with 24 hours (in blue) and 168 hours (in red) central moving average are also plotted in Figure 2-3. There is clearly a big difference between the maximum power for the primary system with and without the moving average.

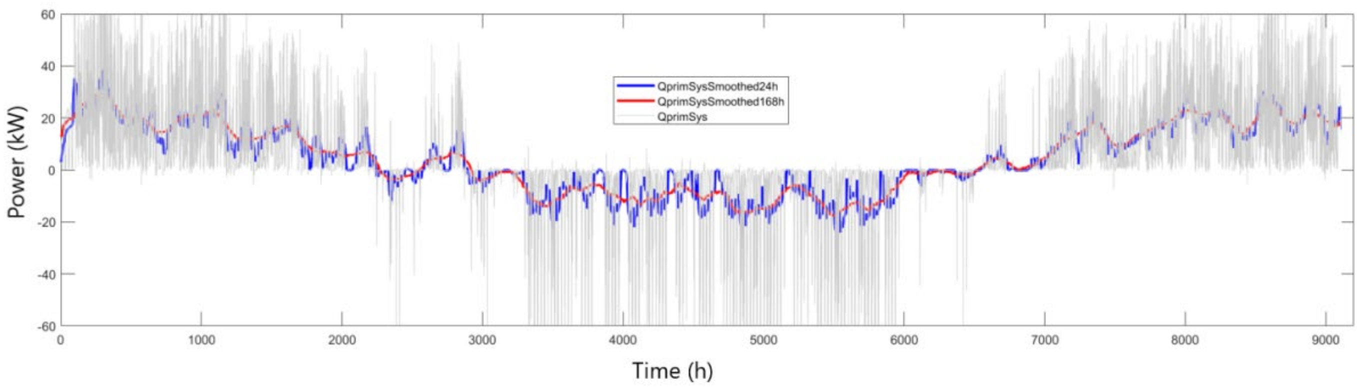


*Figure 2-3 comparison between original and smoothed primary system load*

The question is whether the smoothed signal can provide the thermal comfort in the building as good as the original signal. As there was no way to analytically answer this question and guaranty thermal comfort, the smoothed signal has to be tested for each case study. To test the smoothed signal, the smoothed signal is used as the input to the same RC model as used in the baseload algorithm for each case and the secondary system signal is recalculated to maintain the thermal comfort (this means that in this iteration the optimisation algorithm of the baseload algorithm is not used). If the smoothing has no significant effect on the room temperature, the recalculated secondary system power time series will remain the same as the original signal. Alternatively, if the smoothed signal cannot provide thermal comfort, the secondary system share increases to provide the thermal comfort. Subsequently, the part of the demand that could be compensated by the primary system is taken over by the secondary system. This change is investigated for some case studies and reported below. If in a particular case the change is remarkable, the optimal load split will be adversely effected by the post-processing and the post-processing should not be done for that particular case since the original and optimal load split should not be overshadowed by the post-processing. Yet, there is one question left regarding the smoothing and that is the best time interval for the moving average. This question is also answered in the next section when the influence of the smoothing the primary system time series on energy use and maximum power of each system are investigated.

### The influence of smoothing on the sizing and energy use (case-studies)

In this section we investigate whether the smoothing of the primary system load affects the thermal comfort or shares of primary and secondary system loads, using 9 case studies. The cases are chosen in such a way that variant combinations of the parameters are assessed. To keep the shortness and fluency of the document, the information about the 9 case studies are presented in Annex 1: Case-studies. The flowchart of the post processing consequences evaluation is shown in Figure 2-4. Th procedure enables us to compare the primary system time series before and after smoothing and reveals the influence of smoothing on the secondary system time series. Accordingly the annual load splits can be compared.

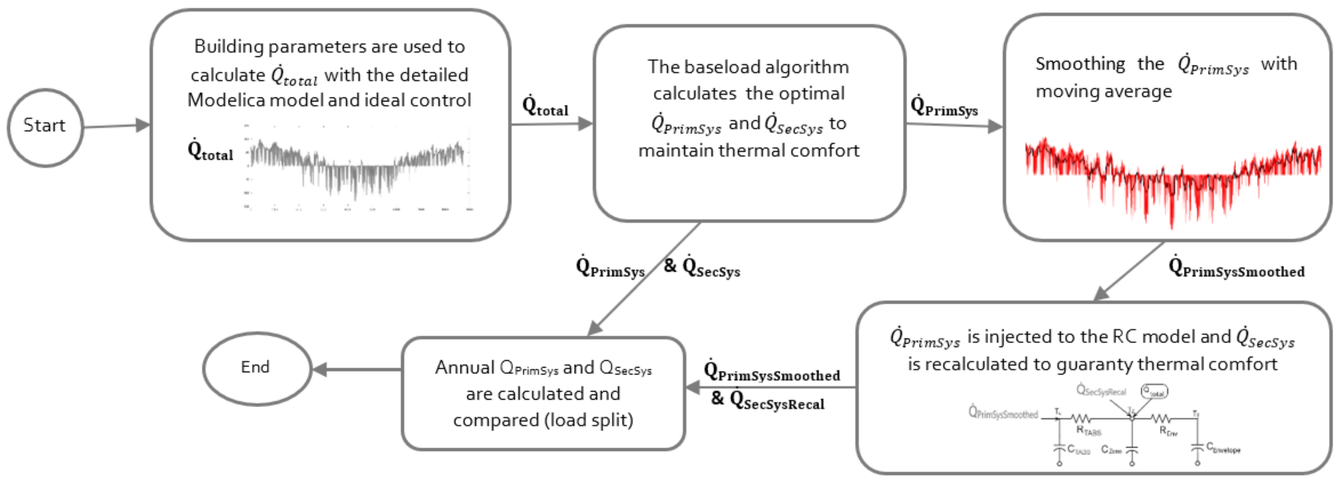

*Figure 2-4 Flowchart of the designed exercise for investigating the moving average influence on load split and sizing of the components*

In the first order of importance we need to know the effect of smoothing on the sizing. As discussed earlier, when using TABS the thermal inertia of TABS should be deployed. This could be done by storing the energy in TABS with a lower rate of heat injection in a longer period rather than using high peaks for the production system in short periods. As mentioned earlier, the maximum load for the primary system is clearly and remarkably different with and without moving average. Therefore, it is expected to have downsizing with smoothing the primary system power time series. On the other hand, the smoothing might increase the share and size of the secondary system. For the 9 case studies, maximum primary and the secondary system in heating and cooling modes with and without the moving average are compared. The comparison is made for different moving average periodicities (the periodicities are 2, 6, 12, 24, 48, 120, and 168 hours, as shown in Figure 2-5). The deviation (vertical axis) is calculated as normalized difference between the maximum load of the primary and the secondary system with and without moving average in the two modes (heating and cooling). Normalisation is made to allow an easier comparison between different cases which have different thermal loads. The normalized deviation for maximum power is calculated using Equation 1:

$$Deviation = \frac{Max(\dot{Q}_{AVGi}) - Max(\dot{Q}_{AVG1})}{Max(\dot{Q}_{AVG1})} \qquad i \in \{2, 6, 12, 24, 48, 120, 168\} \qquad \text{Equation 1}$$

Where the $\dot{Q}$ is the time series of power which is separately considered for the heating (top of Figure 2-5) and cooling modes (bottom of Figure 2-5) for the primary (left side of Figure 2-5) and the secondary systems (right side of Figure 2-5). AVG1 is the time series without moving average and AVGi is the time series with moving average with listed periodicities of i.

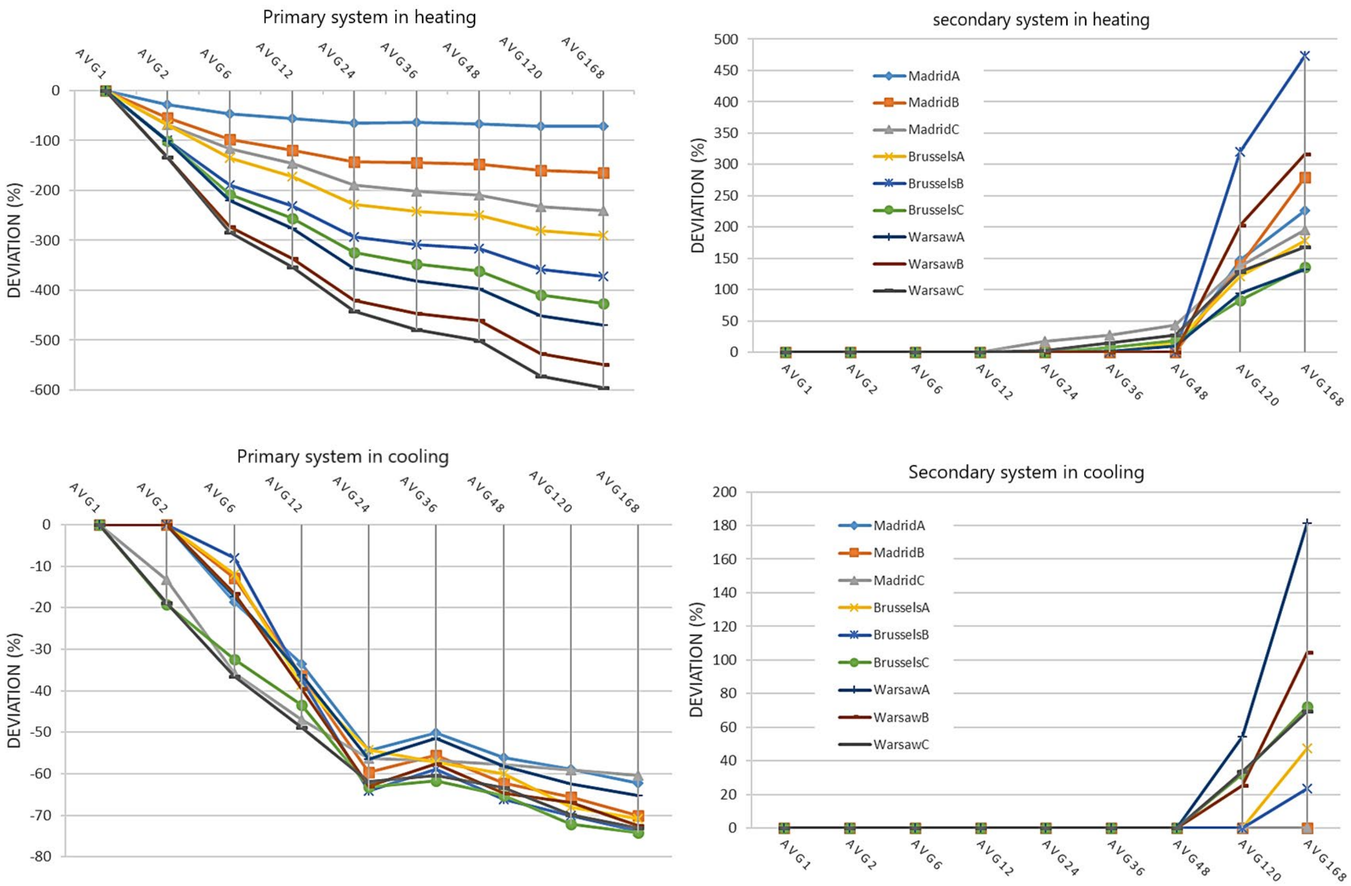


*Figure 2-5 Deviation between **maximum loads** with and without moving average in heating and cooling modes for the primary and secondary systems ( deviation is the difference between maximum loads of the original signal (AVG1) and smoothed signals (AVG2, AVG6,…, AVG168) divided by the **maximum loads** of the original signal (AVG1) to be normalised*

The comparison shows that the smoothing is very effective on the maximum primary system power in heating mode and the slope of lines are more remarkable below AVG24 (Figure 2-5, upper left side). Moreover, in the cooling mode the deviation is more pronounced when the moving average periodicity is lower than 24 (Figure 2-5, button left side). A rather steady behaviour of the lines after AVG24 shows that moving average with lower frequencies (higher periodicities than 24 hours) might not have a high influence on the primary system sizing. As the secondary system size might increase due to the decrease in the primary system size, the comparison is defective if the secondary system maximum loads are not investigated (Figure 2-5, right side ). As seen, except in case MadridC in heating mode for the secondary system no deviation is observed between the maximum of original signal and the recalculated for the periodicities below 24 hours. In cooling mode, the same is seen for the periodicities below 48 hours. Notably, below 48 hours moving there is no difference between the original maximum and recalculated one. This could be due to the essence of the cooling loads which have inherently high fluctuations and the baseload algorithm has already chosen the secondary system for them. Therefore, the smoothing is not effective in cooling mode for the secondary system. However, after AVG48 the increase is observed with an intense slope.

Conclusively, a 24 hour moving average can smooth out the primary system time series effectively in terms of sizing and safely in terms of the secondary system size. The secondary system size in cooling mode is not substantially affected by the moving average. Note that the thermal comfort is ideally maintained in all cases when the temperature is kept within the 22-24 °C. The investigation of the smoothing effect on the results is incomplete if the load split with and without smoothing are not compared (see Figure 2-7). The deviation is calculated as the difference between annual load with and without smoothing divided by the annual load without smoothing for the matter of normalisation.

$$Deviation = \frac{Max(Q^j{}_{AVGi}) - Max(Q^j{}_{AVG1})}{Max(Q^j{}_{AVG1})} \qquad \text{Equation 2}$$

$i \in \{2, 6, 12, 24, 48, 120, 168\}$

$j \in$ {Primary system heating, Primary system cooling, secondary system heating, secondary system cooling}

where Q is the annual load (kWh/year/m²) for the primary or the secondary system in heating or cooling mode. To be able to have a tangible feeling of the amount of heat that are decreased or increased due to smoothing, the load split of the original signal is reported in Figure 2-6, where the relatively small shares of the secondary system are noticed. Figure 2-7and Figure 2-6 together show that the moving average with less than 24 hours periodicity has very little effect on the energy use of the secondary system in heating. For the secondary system in cooling mode negligible effect is seen even with the 48 hour moving average. The 3 cases with C labels show the highest deviation. Looking at the characteristics of these cases (see Annex 1: Case-studies), we know that these are the least appropriate cases for the GEOTABS concept. They are poorly insulated when having high heat gains. Yet, a substantial share of their thermal loads could be efficiently compensated by TABS.

Conclusively, the 24 hours moving average seems safe and effective in terms of load split and sizing of the components. Higher periodicities might not result in much difference and are not safe in terms of optimal load split because they might adversely shift the load towards the secondary system. As seen in Figure 2-6, the maximum share for the secondary system is seen in Madrid C in cooling mode when the secondary system is compensating only 10 % of total cooling demand.

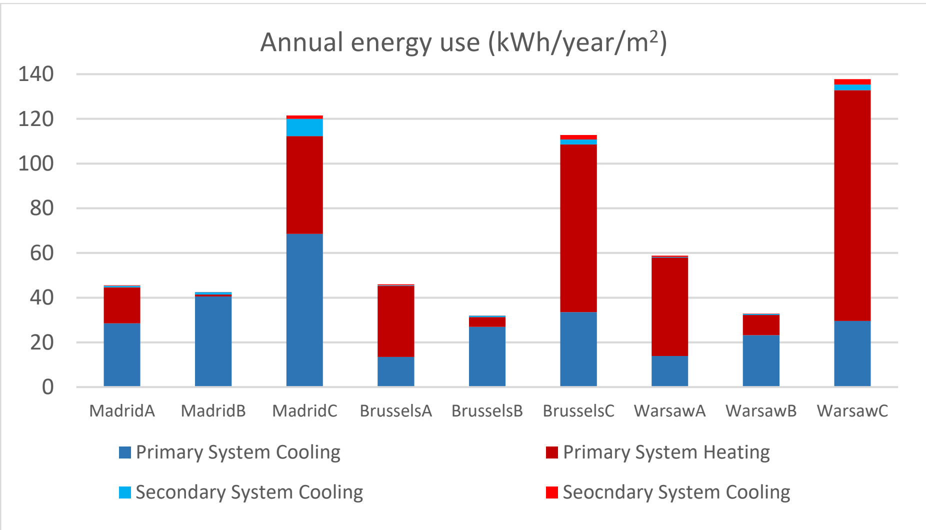

Figure 2-6 Load split with the baseload algorithm for 9 case studies without moving average

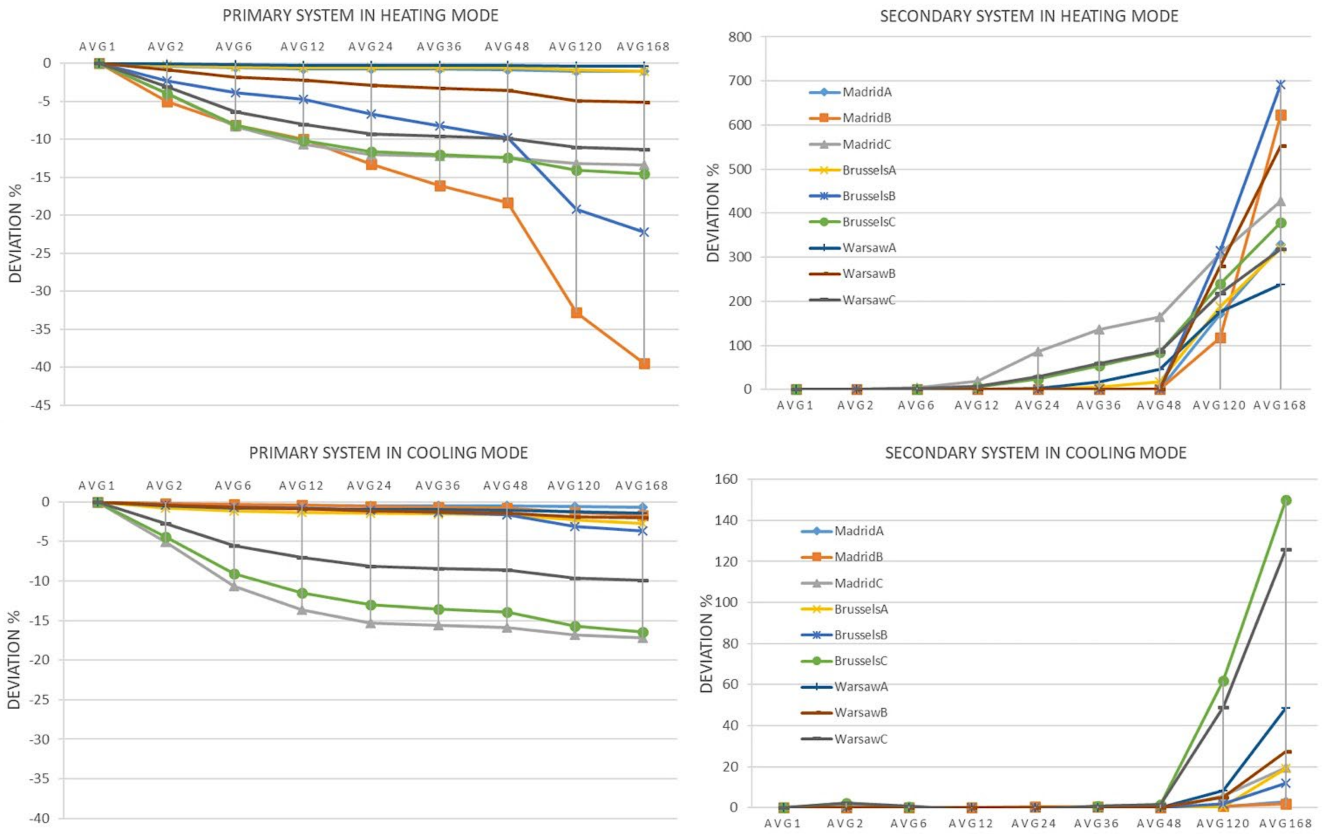


*Figure 2-7 Deviation between **energy use** with and without moving average in heating and cooling modes for the primary and secondary systems ( deviation is the difference between maximum loads of the original signal (AVG1) and smoothed signals (AVG2, AVG6,..., AVG168) divided by the **energy use** of the original signal (AVG1) to be normalized*

## 2.4. From load splitting to sizing: borefield thermal balance

Figure 2-6 already showed that the primary GEOTABS system provides the major part of the heating and cooling demands for the 9 studied cases. Simulation results for all the case studies of the building stock in D2.2 also confirm this finding. As shown in Figure 2-8, more than 75% of office buildings can cover at least 80% of their thermal loads with TABS.

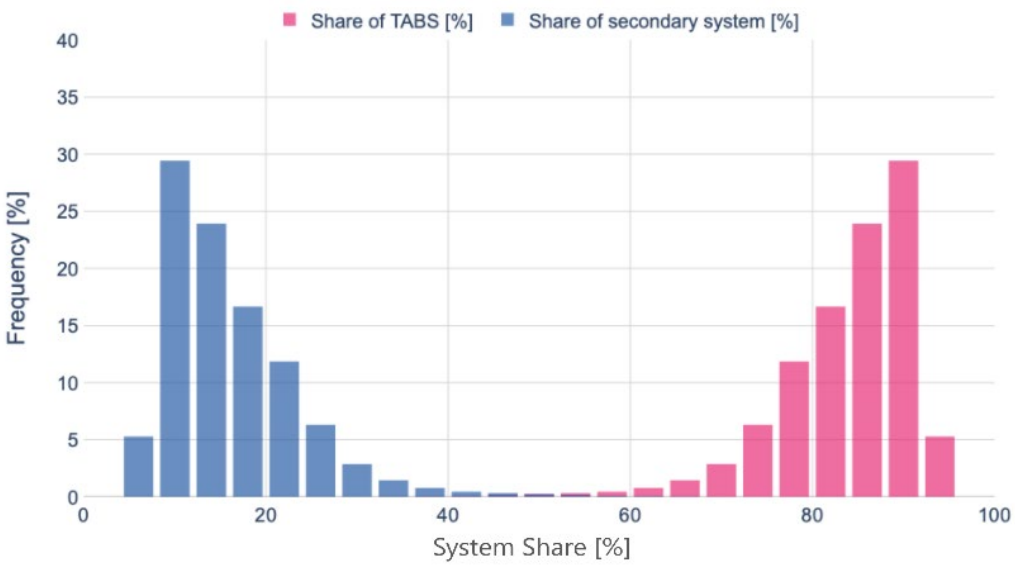


*Figure 2-8 Distribution of the share of the total energy demand that can be covered by TABS in the office buildings included in the database*

The results obtained above can be understood as the maximum share of TABS, but not necessarily the maximum share of GEOTABS, as it is possible that the geothermal source cannot sufficiently fulfil the heating and cooling demands of the building in a sustainable way. For example when there is a severe imbalance between the heat injected and extracted in the borefield on a yearly basis, the temperatures in the borefield could increase or decrease year after year leading to a decreased efficiency. Also there are limitations to the temperatures in the borefield for environmental and technical reasons (e.g. the ground should not freeze).

The behaviour of the geothermal source depends not only on the heat exchange with the building via the TABS, but on many other design parameters, such as the thermal conductivity and properties of the underground, the available area and depth for the borefield, the presence of other geothermal systems nearby and the availability of energy sources to regenerate the thermal balance of the underground. In a more detailed and case-specific design, the designer can play with these parameters to allow for a sustainable design of the geothermal system, taking into account the environmental, energy and financial performance of the designed system.

As the underlying study focuses on the early design stages, and is not aware about the case-specific circumstances in the borefield design, a 'safe' or 'conservative' solution for the geothermal system was chosen, where the geothermal balance is maintained. That is, a balance of the geothermal borefield is imposed on the hybridGEOTABS design, in which the annual heating or cooling load of the borefield cannot be higher than 60% of the total load of the borefield. We call this assumption 'the 40-60 rule' and use it in the final post-processing step of the component sizing, as explained in the next paragraph. As a result, the potential of TABS (without the geothermal balance) and the potential of GEOTABS (with the geothermal balance) provide a more optimistic and a more conservative estimation of the GEOTABS potential, that the designer can choose to further exploit in the further design stages.

### Assumptions for final sizing of components (wrap up the sizing steps)

Here we explain the final steps to provide an automated algorithm for sizing the key components of hybridGEOTABS. First the load duration curves[2] of the primary and the secondary systems are produced (note that the primary system time series after smoothing and the secondary system after recalculating, are used). The next steps are explained by a hypothetical and simplified example as shown in Figure 2-9 and listed below the figure. In this step the secondary production systems are considered as boiler and a chiller for simplicity. This does not take away the fact that the designers can choose other types of secondary systems and their system efficiencies, as long as they use a fast-reacting secondary emission system(s) (e.g. water-based systems such as radiators and convectors, or air-based emission systems).

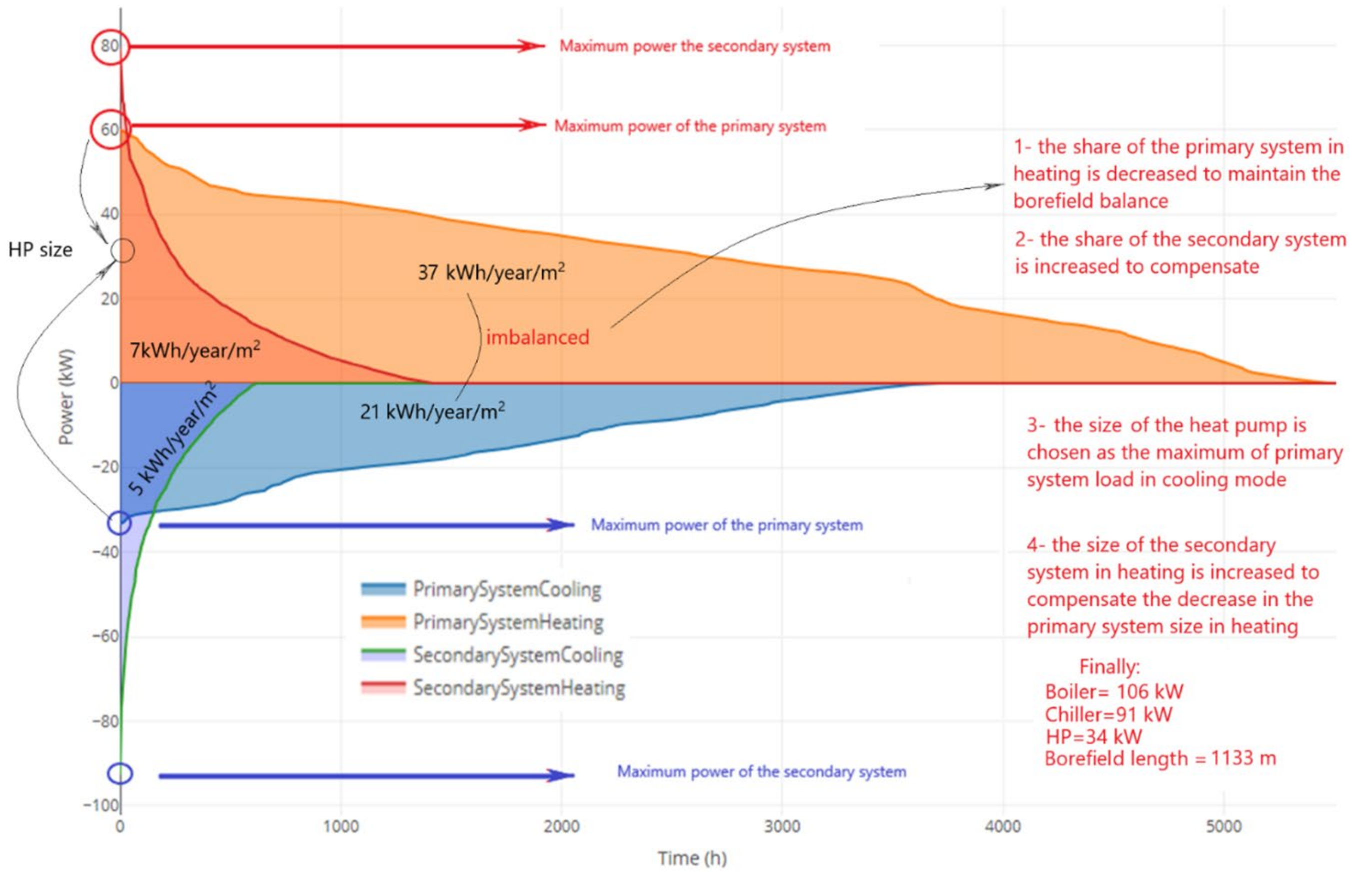


*Figure 2-9 load duration curves for the primary and secondary systems in heating and cooling modes for a hypothetical example. The steps of final sizing are mentioned inside the figure*

[2] Load duration curves are the time series which are sorted from the maximum to minimum load allowing us to see the maximum of the load and its behaviour throughout the year

1. The maximum power of the primary and the secondary system in heating and cooling are considered as the ***initial guess*** for sizing. Note that to choose the maximum ***primary*** system in heating and cooling we eliminate the first 25 maxima (first 25 hours in the load duration curve) because the curve might be too steep in that region and we don't want to choose the primary system size based on the maximum that happens very rarely. This is not shown in Figure 2-9 to keep the figure clear.
2. The primary system loads are converted to the borefield load considering the COPs. Constant COPs are assumed for heating and cooling separately, for heating $COP_h$=6, for active cooling $COP_c$=5, and for passive cooling $COP_c$=20. In the Mediterranean climates, represented by Madrid, 100% active cooling is assumed. In the central and northern European climates, which are represented in this document as Brussels and Warsaw, it is assumed that only passive cooling is used. Note that in passive cooling the heat pump is not used but the COP is calculated considering the electricity use of the circulation pumps only. To check how the COPs are applied for calculating the borefield load, refer to Kavanaugh and Rafferty (2014) [8, page 53]
3. If the borefield thermal balance is maintained (according to the '40-60 rule', as introduced above) the initial guess is reported as the final sizing. If not, the share of GEOTABS is decreased so that the balance is maintained and the secondary system compensates the decreased part instead of GEOTABS. In this case the sizing has to be continued to ***resize*** the systems according to the new share for the primary and the secondary systems. The resizing happens as follows:
    a. The heat pump size, after maintaining the balance, equals to the smaller maximum power in cooling and heating modes. If the chosen heat pump power is smaller than the maximum primary system load in one mode, the secondary system size in that mode is increased to compensate.
    b. In both modes, the secondary system size is increased as much as the primary system size was decreased in the previous step.
4. The size of the geothermal borefield is approximated with the heat pump size in southern European climate. While, in the central and northern European climate the borefield is sized with maximum cooling load to be able to use passive cooling. The borefield length is approximated with the conservative assumption of 30 W/m for the borefield.

All the aforementioned steps are translated to an algorithm and accordingly to a MATLAB code to be applied on all the cases of the database and calculate the size of all key components automatically. The algorithm is shown in Figure 2-10.

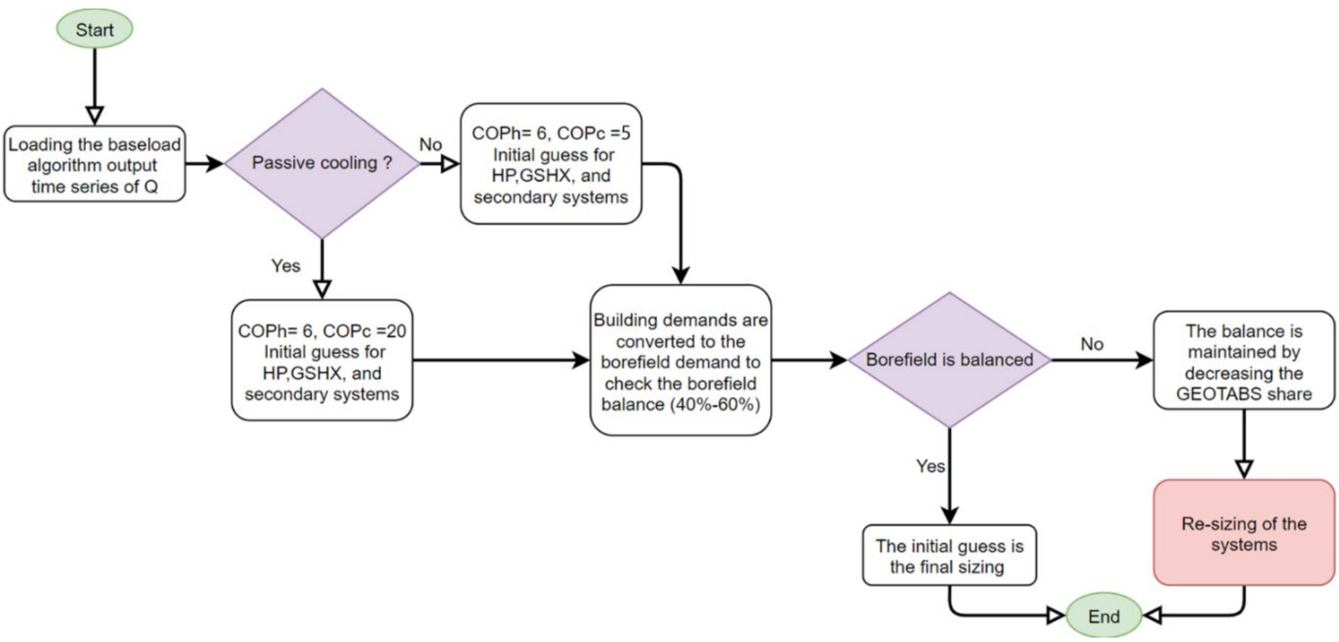


*Figure 2-10 the algorithm for final sizing of the hybridGEOTABS components*

## 2.5. Performance estimation

The heating and cooling demands (after balancing) for the primary and secondary systems are used to calculate the final energy use of the building (using the efficiencies in Table 2-1) per energy source, and the primary energy and $CO_2$ emissions (using the conversion factors Table 2-2).

*Table 2-1: Production efficiencies for the different systems*

| *Type of production unit* | *efficiencies* |
|---|---|
| *Heat pump (heat production) SPF* | *6.00* |
| *Heat pump (Cold production) SPF* | *5.00* |
| *Gas boiler (heat production)* | *0.95* |
| *Electric chiller (Cold production) EER* | *3.00* |
| *Passive cooling (Cold production)* | *20.00* |

*Table 2-2: Primary energy and CO2 emission conversion factors*

| | *PE Total (-)* | *$F_{CO_2}$-emissions (g/kWh)* |
|---|---|---|
| *Natural Gas* | *1.1 (ISO520000-1, 2017)* | *220 (ISO520000-1, 2017)* |
| *Electricity EU 2020* | *2.0 (Hamels, 2020)* | *260 (Hamels, 2020)* |

## 2.6. Wrap-up

In this section the algorithm for sizing the key components of hybridGEOTABS was explained. The algorithm starts from the post processing of the baseload algorithm outcomes. The necessity and importance of the post processing were elaborated first. Then the post processing approach which is smoothing the primary system time series was introduced. The consequences of the post processing were discussed and the methodology for avoiding probable adverse effects of the post processing was explained and validated. Afterwards, the final steps for sizing the key components were elaborated. As the long term borefield thermal balance is considered a crucial aspect of the system to keep it sustainable, a conservative assumption was taken to guaranty the thermal balance. The assumption is called 40-60 rule meaning that the annual thermal load of the borefield in any of the heating or cooling modes cannot be lower than 40% (or similarly higher than 60% ) of the total annual demand. In the next section the entire methodology is applied on 5 case studies and validated against the results of an optimal and detailed but time consuming sizing methodology developed in T2.3. The whole sizing procedure then is translated to an automated code and applied on over 140,000 pre-simulated case studies. Finally, design decision trees and accordingly design guidelines are derived from meta-analysis of the whole dataset. The flowchart of the entire procedure and different steps is depicted in Figure 2-11.

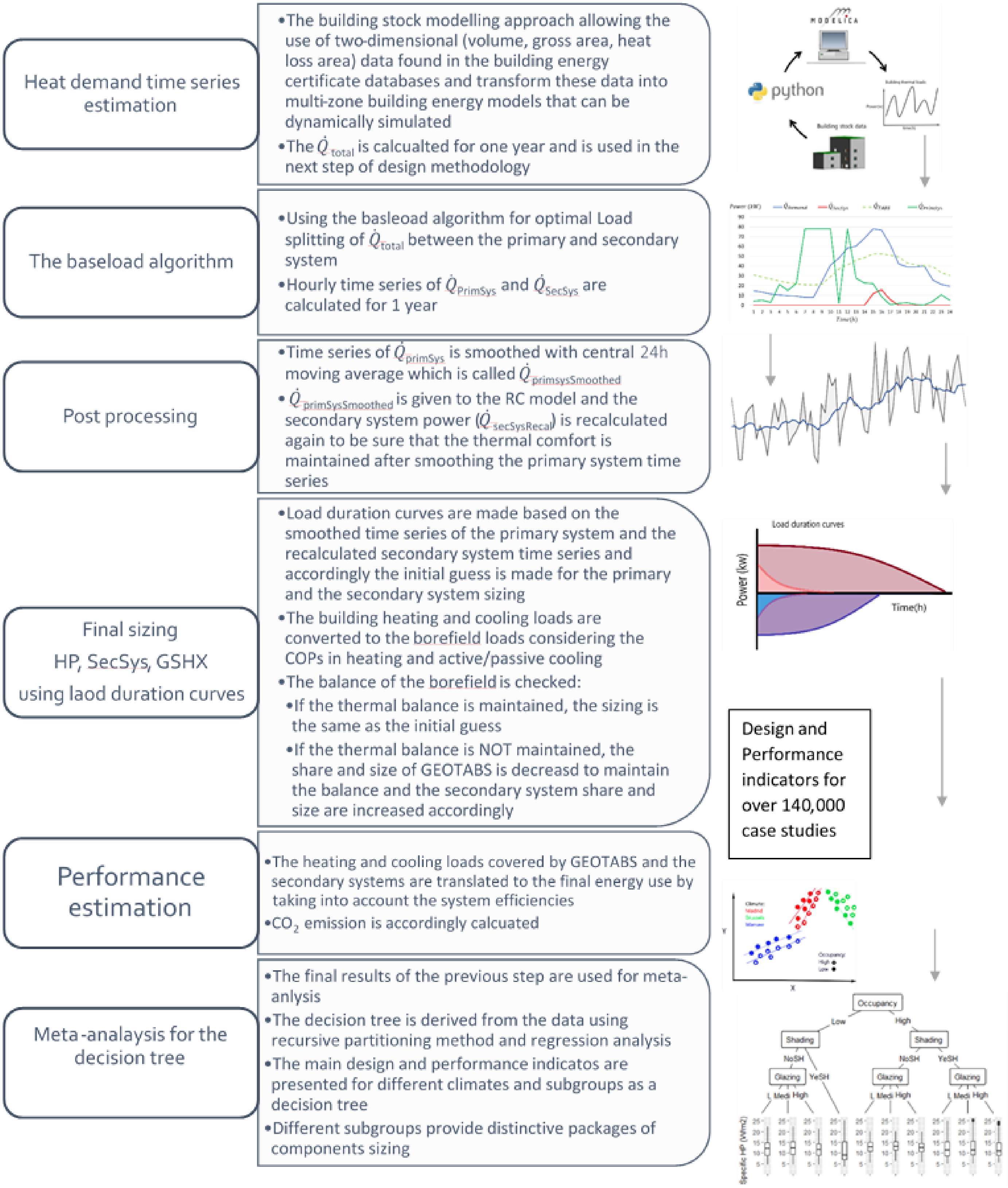


*Figure 2-11 Flowchart of the different steps taken in work package 2 of the project for going from the building stock analysis to the design guidelines and the design decision trees of the key components of hybridGEOTABS*

# 3. Verification with detailed control-integrated design results

In this chapter, the outcomes of the final sizing algorithm (as introduced Chapter 2) are compared to the outcomes of the more detailed (but more calculation-intensive) control-integrated design algorithm as developed in T2.3 of the project, for selected case-study buildings. In D2.4, the more detailed algorithm was applied to 5 case-study buildings, and for each of the them key component sizing and energy performance were estimated assuming the use of rule-based control (RBC) and model predictive control (MPC). The same five case-study buildings are used in this chapter and their properties are documented in Annex 1: Case-studies.

Figure 3-1 shows the sizing of the heat pump (HP), the boiler (which is the secondary system for heating) and chiller (which is the secondary system for cooling) as results of the detailed algorithm with *RBC* and with *MPC*. Furthermore, it shows the sizing results of the final sizing algorithm, including the baseload algorithm without and with applying the borefield balance assumption (as introduced in section 2.4), respectively called *BA-Imbalanced* and *BA-Balanced*. $Q_{design}$ represents the maximum steady state thermal load of the building for heating and cooling, estimated according to the calculation method documented in Annex 1: Case-studies.

These results allow to make a 'sanity check' of the newly developed load splitting and sizing algorithm, as well as to investigate how the thermal balance assumption (see chapter 2.4) affects the sizing outcomes.

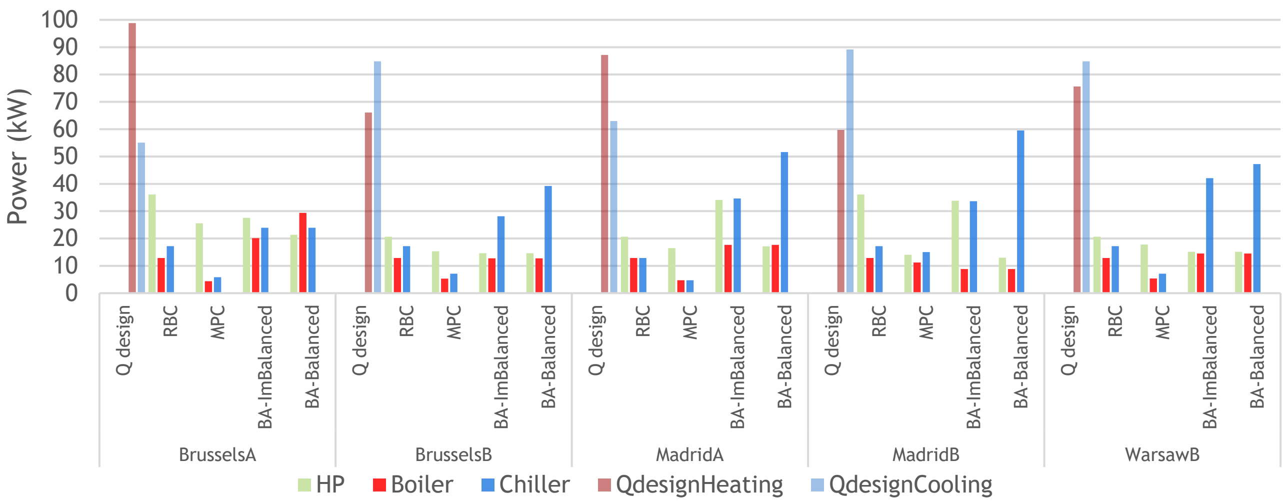


*Figure 3-1 Component sizing comparison between MPC and RBC scenarios from D2.4, and BA with and without applying the balancing assumption ($Q_{design}$ is the maximum steady state building demand in heating and cooling)*

Observing the results in Figure 3-1, a remarkable difference between the $Q_{design}$ and the components sizing with all the variant approaches is observed, showing an overestimation of the required component sizing by the steady-state calculation method. The heat pump size with *BA-ImBalanced* is found to be close to the MPC scenario for the cases in Brussels and Warsaw, and closer to the RBC scenario for the two cases in Madrid. However, the sizing based on the baseload algorithm typically leads to a larger sizing of the secondary systems in comparison to MPC and RBC scenarios[3], especially for the secondary system in cooling. Comparison between

[3] Note that in the detailed control-integrated design method the thermal comfort bounds are considered 21-25 °C. However, in the early design stage with baseload algorithm the thermal comfort bound is considered 22-24 °C. This will lead to a more conservative (larger) sizing and will mainly influence the secondary system size because TABS is not normally used to keep the zone temperature at the borders of the thermal comfort bound but within an acceptable range. This explains the overestimation of the secondary system with BA.

the balanced and imbalanced scenarios shows that by applying the borefield balance assumption, in which parts of the load are shifted to the secondary system, its size also increases.

Figure 3-2 shows the annual load splitting into GEOTABS and secondary systems for heating and cooling, for the different methods and cases. It is clear that the load splitting obtained by the baseload algorithm, allowing thermal imbalance of the borefield, is most similar to the outcomes of the detailed methodology with MPC, which confirms the good performance of the baseload algorithm. The RBC, MPC and the imbalanced BA lead to high shares of GEOTABS in the load splitting. The significant influence of the borefield balance assumption is clear when comparing the BA-Imbalanced and BA-Balanced results. For example, cases Brussels B and Madrid B have very high cooling loads and very small heating loads, resulting in a very low share for the primary system when the borefield thermal balance assumption is applied, which also explains the increased sizes of the secondary cooling system. However, a low heating demand does not imply that no heating system is required. Load duration curves of heating and cooling loads of the primary and the secondary system are useful to make the decision (load duration curves of these case are documented in Annex 1: Case-studies). Note that these cases B have a very high insulation level (passive house) and high internal heat gains. Especially in a warmer climate like Madrid, this combination is problematic. Such building design is of course rather exceptional in reality, but its investigation is of interest for testing the sizing methodology. On the other hand, cases like BrusselsA, naturally have a better balance between heating and cooling and expectedly have higher shares for the GEOTABS.

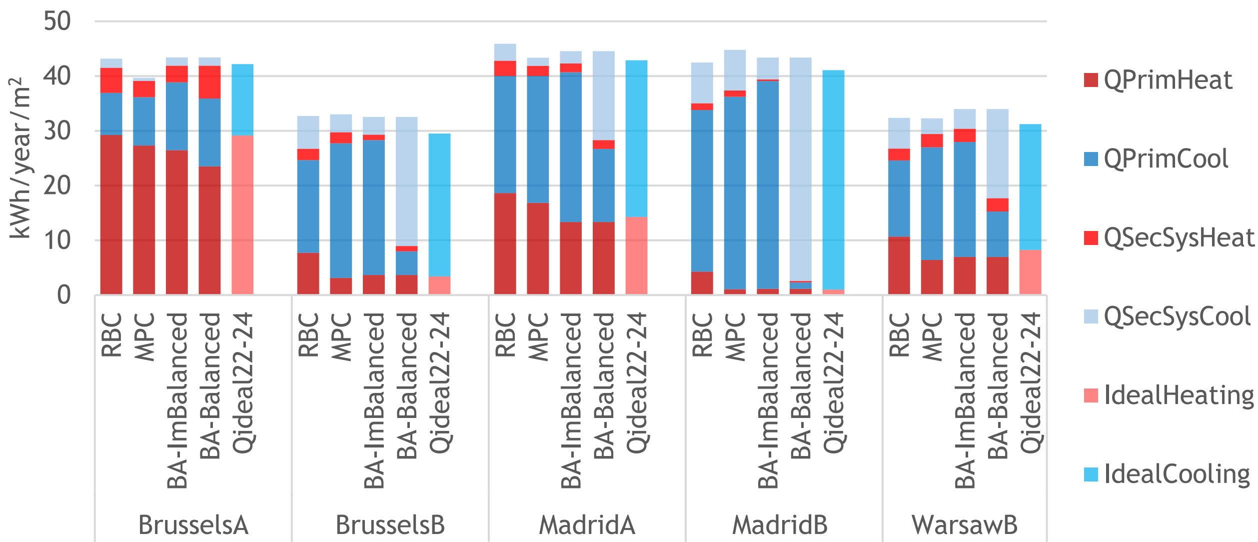


*Figure 3-2 Annual load split with different methodologies, MPC and RBC from D2.4, BA with and without applying the balancing assumption*

The balancing effect is also observed when observing the borefield length estimations in Figure 3-3, showing a decrease in borefield length for the BA-Balanced scenarios, as they have lower shares of GEOTABS. It is observed that the borefield size under BA-Imbalanced scenario is close or higher than MPC and RBC scenarios except for BrusselsA.

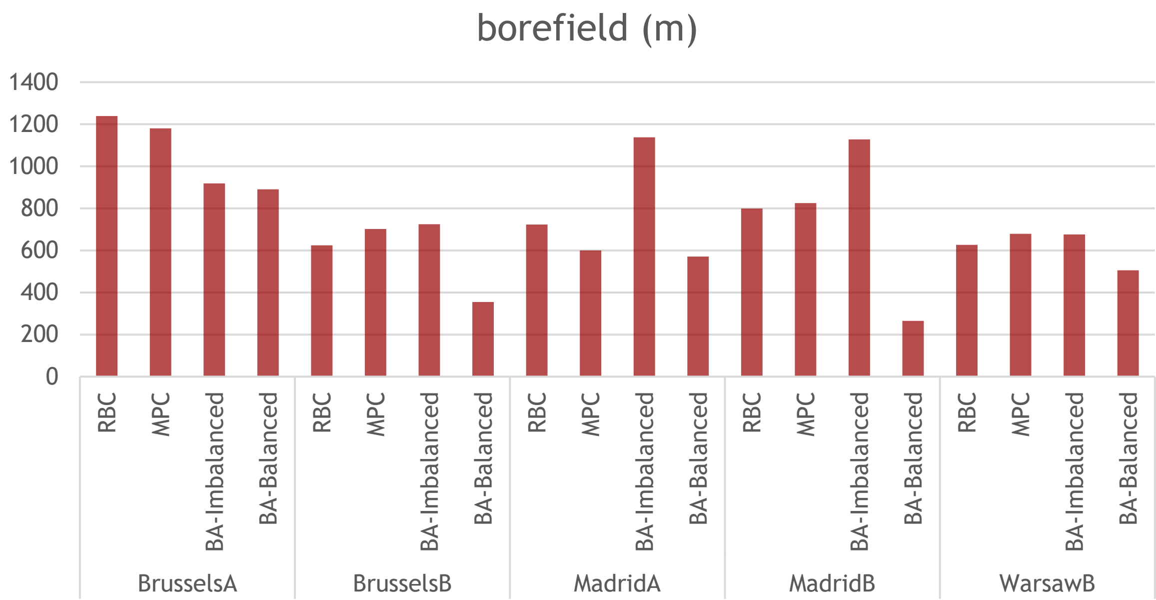


*Figure 3-3 comparison of the borefield length with different approaches, MPC, RBC,. BA-Balanced, and BA-Imbalanced*

From this comparison it can be carefully concluded that the fast sizing method based on the baseload algorithm is able to arrive to a sizing and load splitting in the same order of magnitude or on the 'safe side' of the more detailed control-integrated design method. Its results are most similar to those of the detailed method with MPC, which makes sense as the baseload algorithm also implements a predictive type of controller (see D2.1).

Regarding the borefield balancing, it is noted that the load splitting as obtained by the more detailed design methods with RBC and MPC, which do include a constraint on the borefield thermal balance[4], are most closely approached by the BA-Imbalanced results. This indicates that the borefield balancing assumption (40-60) leads to a much more conservative estimation of the sizing and performance. In this regard, the outcomes of the pre-design methodology can be understood as 'cautious' results, which fit in this early stage of the design where the HVAC-designer rather wants to be on the safe side, and may not be aware yet of the limitations of the geothermal borefield. From this point of view, the balanced results can be understood as a 'minimum' share of GEOTABS that is possible. At the same time, it confirms the usefulness of the imbalanced outcomes of the load splitting algorithm, that represent the further optimisation potential of the design after a dedicated study of the geothermal borefield design, and possibly including borefield regeneration solutions. Finally, the importance of the sustainable building design is also pointed out with the presented data. The building should be designed in a way that a thermal balance is maintained between heating and cooling loads.

[4] As introduced in D2.4 (section 2.1), the borefield behaviour is modelled over a 25 year period, and its thermal balance has to be maintained.

# 4. Results

The algorithm for sizing of the key hybridGEOTABS components as explained in chapter 2, was translated to an automated software code that calculates the share of GEOTABS and the secondary system and the nominal power of the components from the total annual heating and cooling load for all the cases of the building stock database. As mentioned earlier the database contains about 140,000 building cases. This section provides insights in the overall sizing-related outcomes, taking all the ca. 40,000 cases from the office building typology as example.

## 4.1. GEOTABS share

Figure 4-1 illustrates the distribution of the share of the heating and cooling loads covered by the GEOTABS system for the office building cases. Roughly more than half of cases have more than 50% share of GEOTABS, but there are also cases with a much smaller share of GEOTABS. Figure 2-8, that shows the GEOTABS share before the balancing of the borefield (the '40-60 rule') and the final sizing steps are applied, demonstrated GEOTABS shares of more than 75% for the majority of the cases. When comparing to Figure 4-1 it is clear that the limitations of the GEOTABS share are an effect of the balancing assumption. Thus, Figure 2-8 and Figure 4-1 are showing an optimistic and a more conservative estimation of the GEOTABS potential in buildings. Using the final design guidelines, as proposed in chapter 5, the designers/architects can select the more suitable building designs for having higher shares of GEOTABS as a sustainable solution.

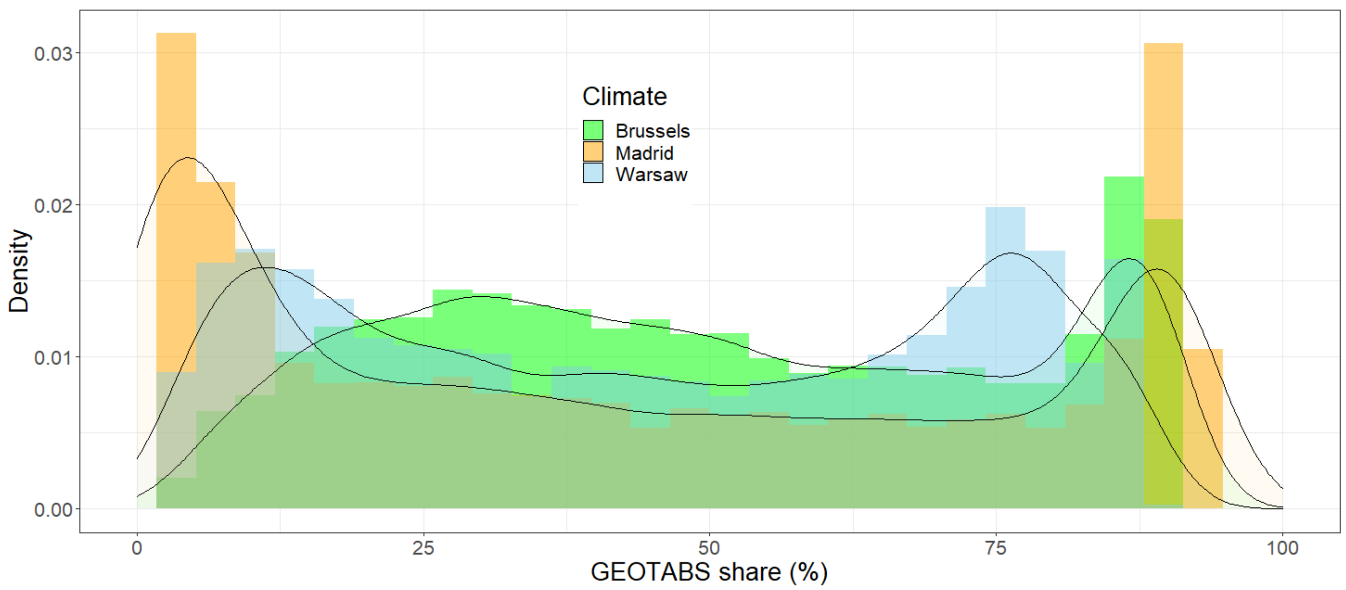


*Figure 4-1: Distribution of the share of the total energy demand that can be covered by GEOTABS in the office buildings included in the database*

## 4.2. Sizing

Figure 4-2 shows the distribution of the absolute size of the key components in the office stock: the heat pump (HP), the secondary system in heating (boiler) and secondary system in cooling (chiller). The distribution for the heat pumps appears more dense than for the other components. The chiller has the highest deviation showing that probably choosing the optimum size of the chiller might be more difficult than for the other components. Note that the distributions of the absolute powers are highly affected by the total conditioned area of the cases which ranges between 1,000 m² and over 20,000 m², with a majority of the cases having floor areas below 5,000 m² (see D2.2). In Figure 4-3 the distribution of nominal heat pump power per climate zone is presented, showing that the highest density is for small heat pumps below 25 kW. Note that these sizing results are obtained after balancing, and thus also include cases with low GEOTABS shares.

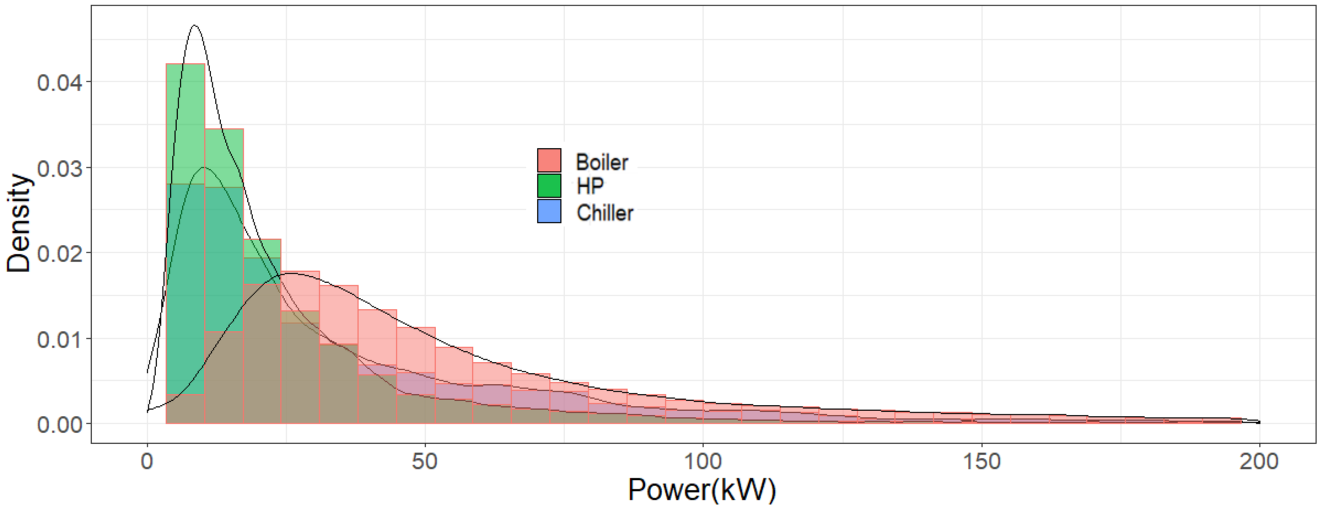


*Figure 4-2 Distribution of the nominal power for HP, boiler and chiller in office cases*

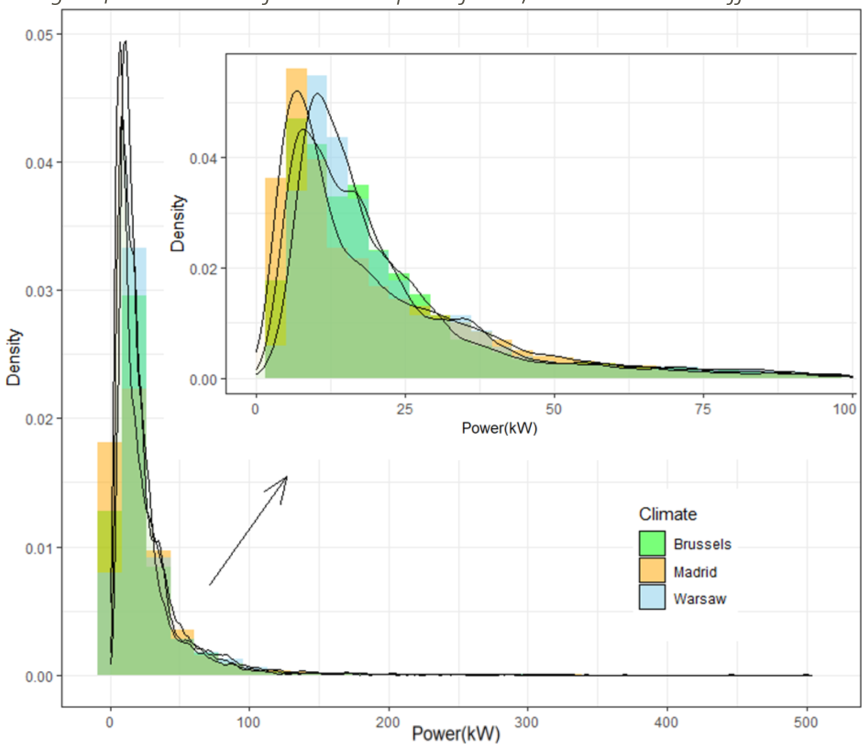


*Figure 4-3 Distribution of the HP power as the output of the sizing methodology for the office cases*

Figure 4-4 gives the specific HP power (the heat pump power per m² of conditioned floor area) distributions per climate zone, showing the differences between the climatic zones more pronounced. The specific heat pump power also is a more suitable parameter to relate to parameters such as climate, insulation level, occupancy, etc. (parameters are defined in D2.2 and Annex 3).This is done in Figure 4-5, where the climate, insulation level and occupancy type are used as parameters. We learn that when the insulation level is high, the deviation in the specific HP power is low for both high-dense and low-dense occupation. The influence of occupation on the sizing is more obvious in the cases with low and medium insulation levels. The highest specific powers are observed for the low-insulated building cases in Madrid. The violin plots for the medium insulated cases prove that the design for high and low dense occupancy is different despite the fact that the box plot shows a symmetrical distribution in one group. As another example, with high dense occupancy for medium insulated cases in Brussels, the graph shows two distinct groups.

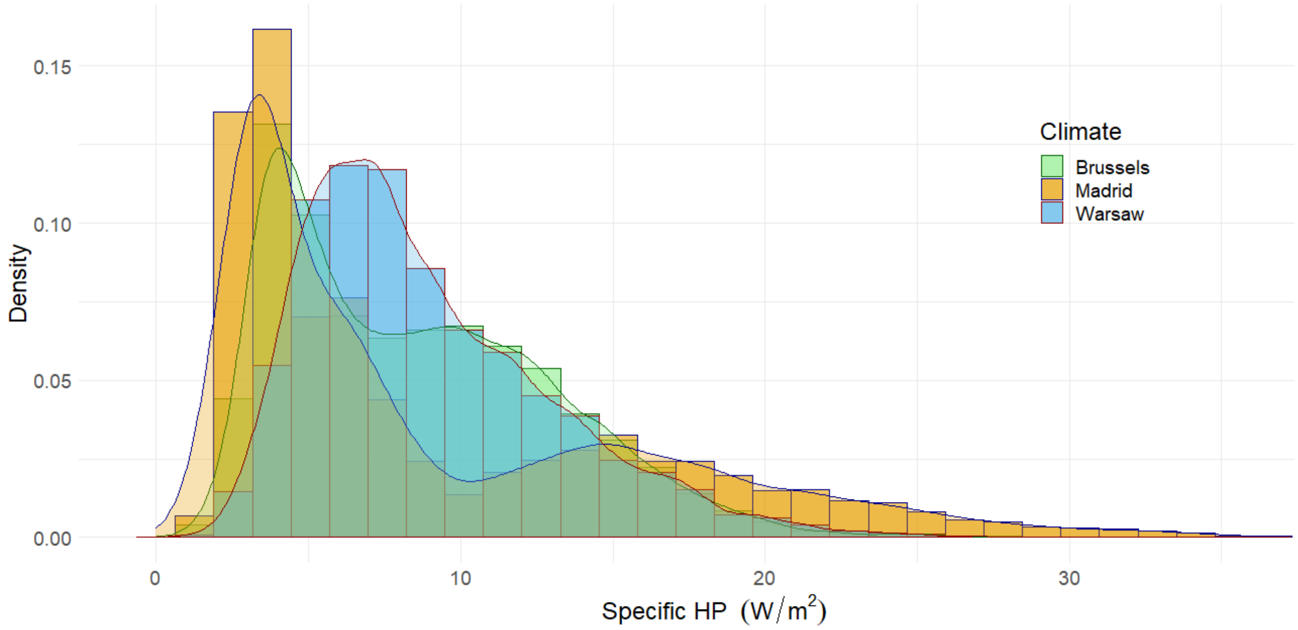


*Figure 4-4 Distribution of the specific HP power in office cases*

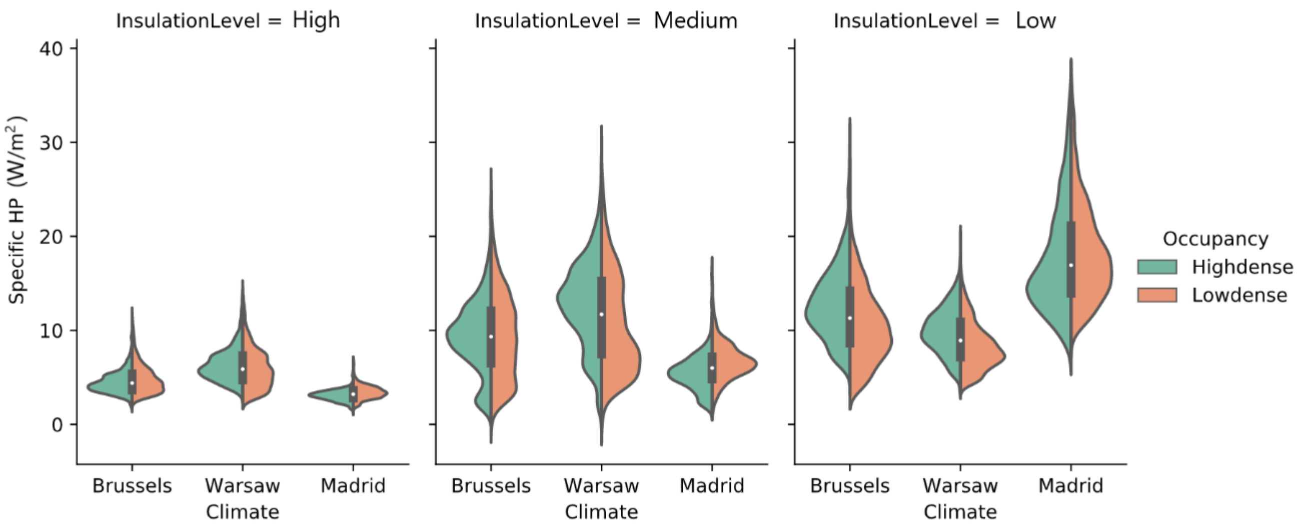


*Figure 4-5 Distribution of the specific maximum HP power in office cases related to different design parameters*

These high-level observations confirm the relationship between the specific sizes of components and the building energy-related design characteristics. A further analysis and statistical testing of the relationships between these characteristics and the specific sizes and performance of hybridGEOTABS designs, is the starting point for the development of design guidelines, helping designers in the earliest design stages.

In the design guidelines developed in the next chapter, the conditioned floor area is used for normalising the component size (W/m²), because this is one of the key parameters that is most easily available in the early building design documentation. An alternative would be to relate the component power to the standardised steady-state design load calculation, $Q_{design}$, for which a methodology is provided in Annex 2. For example, Figure 4-6 shows that when the data are partitioned into groups of properties, different and more specific and accurate regression lines (models) are derived using statistical methods. Although not being the objective of the current study, the development of a design methodology that relates the hybridGEOTABS sizing to the $Q_{design}$ estimations is an interesting path for further research.

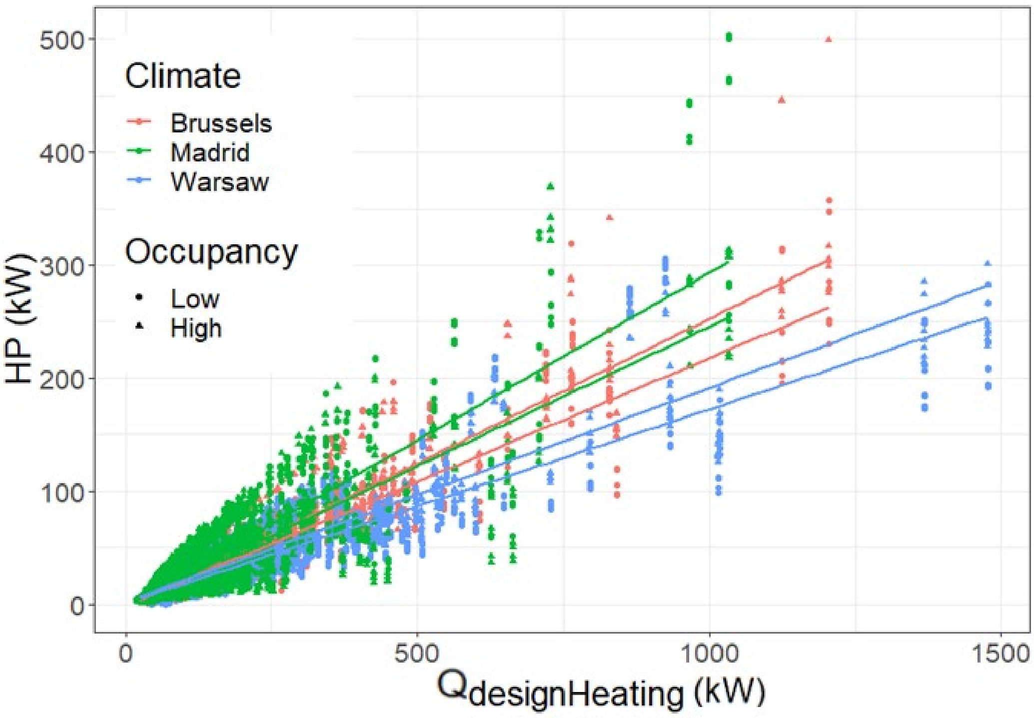


*Figure 4-6 Difference between different regression lines for different groups according to subgroups*

# 5. Sizing guidelines

## 5.1. Methodology for data analysis

In the previous chapter insights for analysing the outcomes of the automated sizing algorithm were introduced, based on exploration of the office building results. In this section, an approved and automated algorithm for exploring the most relevant outputs of all the building cases, with the aim of providing the design guidelines, is explained.

To find the subgroups in the data, first a variable is chosen and the data are split (branches). Next, the portioning into subgroups is continued until the level of achieved accuracy of the regression line of each branch is accepted. This methodology is called "recursive partitioning" because the partitioning is done recursively throughout the whole dataset considering the predictors [9, 10]. The final outcome will be a decision tree whose final groups are the fitted regression lines for subgroups (Figure 5-1). The difference between final groups are statistically significant while cases within each group are not significantly different.

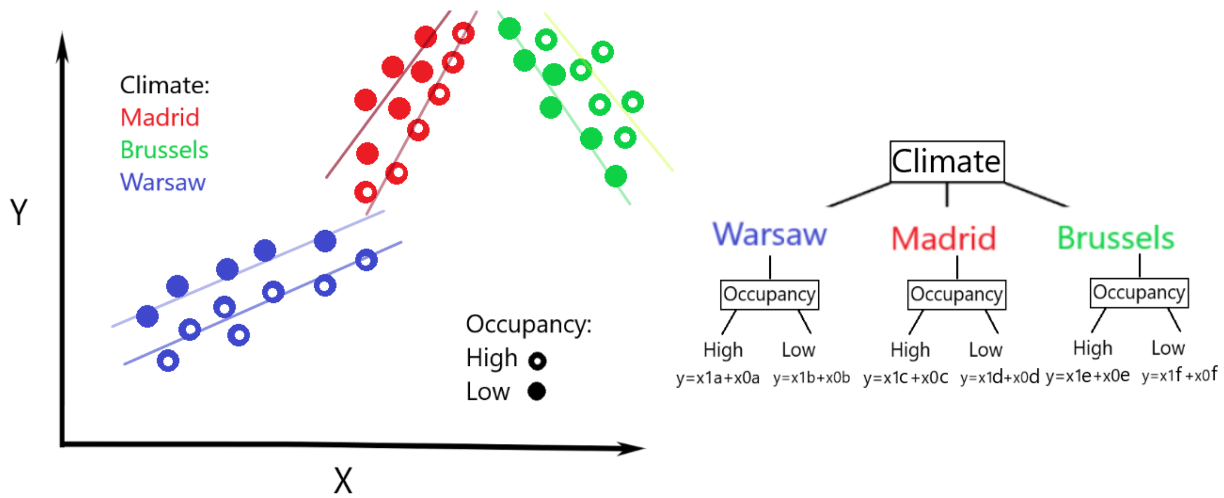


*Figure 5-1 Partitioning algorithm leading to a decision tree*

To apply the methodology to the dataset automatically, an R code was developed and the function "*ctree*" from the package "*partykit*" is used [9]. The function *ctree* builds the tree by applying statistical tests on the dataset. It finds the optimum split based on a greedy algorithm looking for the variable that meets the growing criterion better than the other variables in each step. For each subgroup, first the p-value is calculated. If subgroups have significant p-values they are considered as separated groups and thus the tree grows. In each step, the variable that has the highest influence on the output is chosen as the root. The function has different stop criteria to stop growing the tree at a certain point. As a matter of fact, a bigger tree always brings more accuracy. However, the interpretation of such big tree is not easy and the amount of branches can become considerable. Therefore there is trade-off between the size of the tree and the achieved accuracy, taking into account the presentation format of the tree. Normally the function stops when the p-values are not significant or if the null-hypothesis is rejected. However, in our dataset the p-values are significant even for the smallest subgroups because the dataset is very large. Even the *Bonferroni* correction could not help to have more meaningful p-values. Considering the main target of developing the decision tree, we aimed at a rather small and easily accessible decision tree. Therefore, we manually controlled the decision tree development. First, the stop criterion is chosen as the size of tree to prevent having a big tree. Moreover, to keep consistency between different decision trees of different typologies, the same order of the parameters to split into branches are imposed to the function for all the trees, after studying the influence of the various parameters.

As a result, in all typologies, the order of variables are as follows: climate, insulation level, glazing area, shading, and occupancy. The order is chosen based on the investigations on the outcomes of different decision trees developed by the algorithm. In the next section, the outcome of the tree with and without the manual controls are compared and explained.

## 5.2. Decision trees as design guidelines

In this section, first we show the outcome of the partitioning algorithm according to the *ctree* function. Then we show and compare the outcomes of the tree with manually chosen order of the variables common for all typologies. Finally, with some examples we guide the reader how the final decision trees can be used for sizing the key components of hybridGEOTABS. Also, we compare the outcomes with the case studies previously introduced and investigated in this document.

The partitioning algorithm finds the local optima for splitting and thus the branches are not necessarily the same throughout the tree (Figure 5-2). For instance, in medium-insulated buildings the glazing area comes after insulation level as the most important predictor, while in low-insulated buildings occupancy is found more important. This makes the tree hard to follow considering that in total there are four trees (for four typologies and three climates) and the different tree structures might confuse the user. Therefore, it was decided to have a uniform decision tree in the format that is shown in Figure 5-3. This makes the trees much more user-friendly. The order of variables are chosen based on the investigations coming from the algorithm outputs in such a way that the most effective variables are coming first. Moreover, considering all the indicators that should be delivered to the designer, the visualization of the trees cannot be as the classic way in Figure 5-3 but as in Figure 5-4.

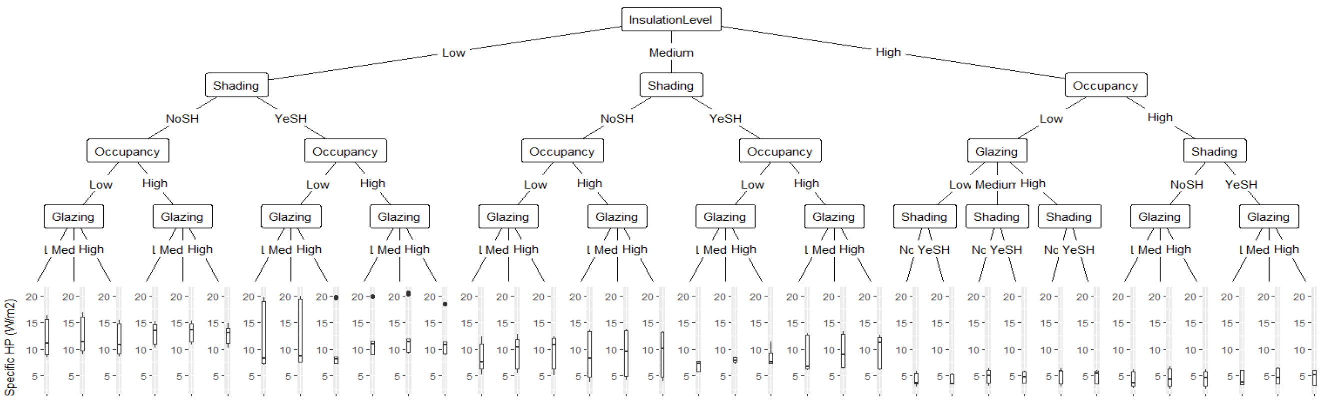


*Figure 5-2 Developing the decision tree for office cases in central European climate (Brussels) using **ctree** function*

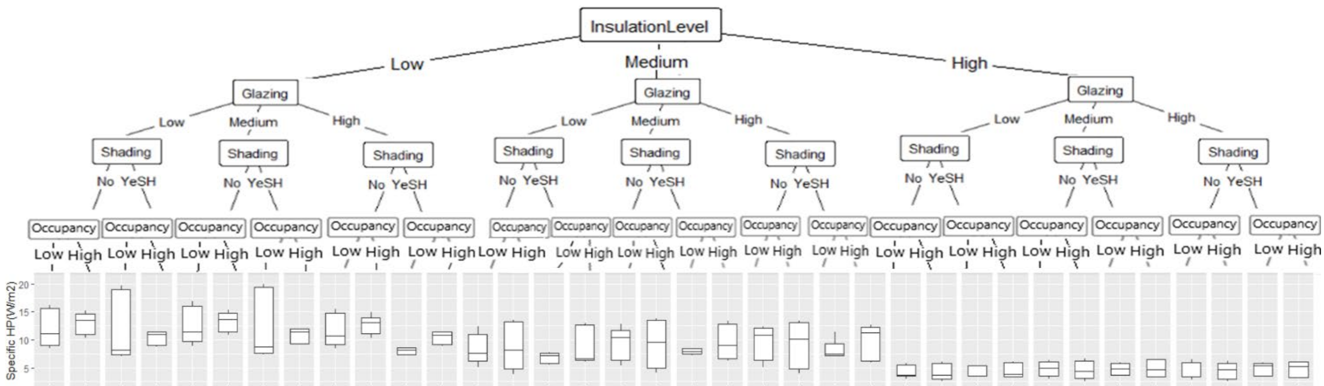


*Figure 5-3 Decision tree with manually chosen variables as predictors for office cases in central European climate (Brussels) with imposed order of variables*

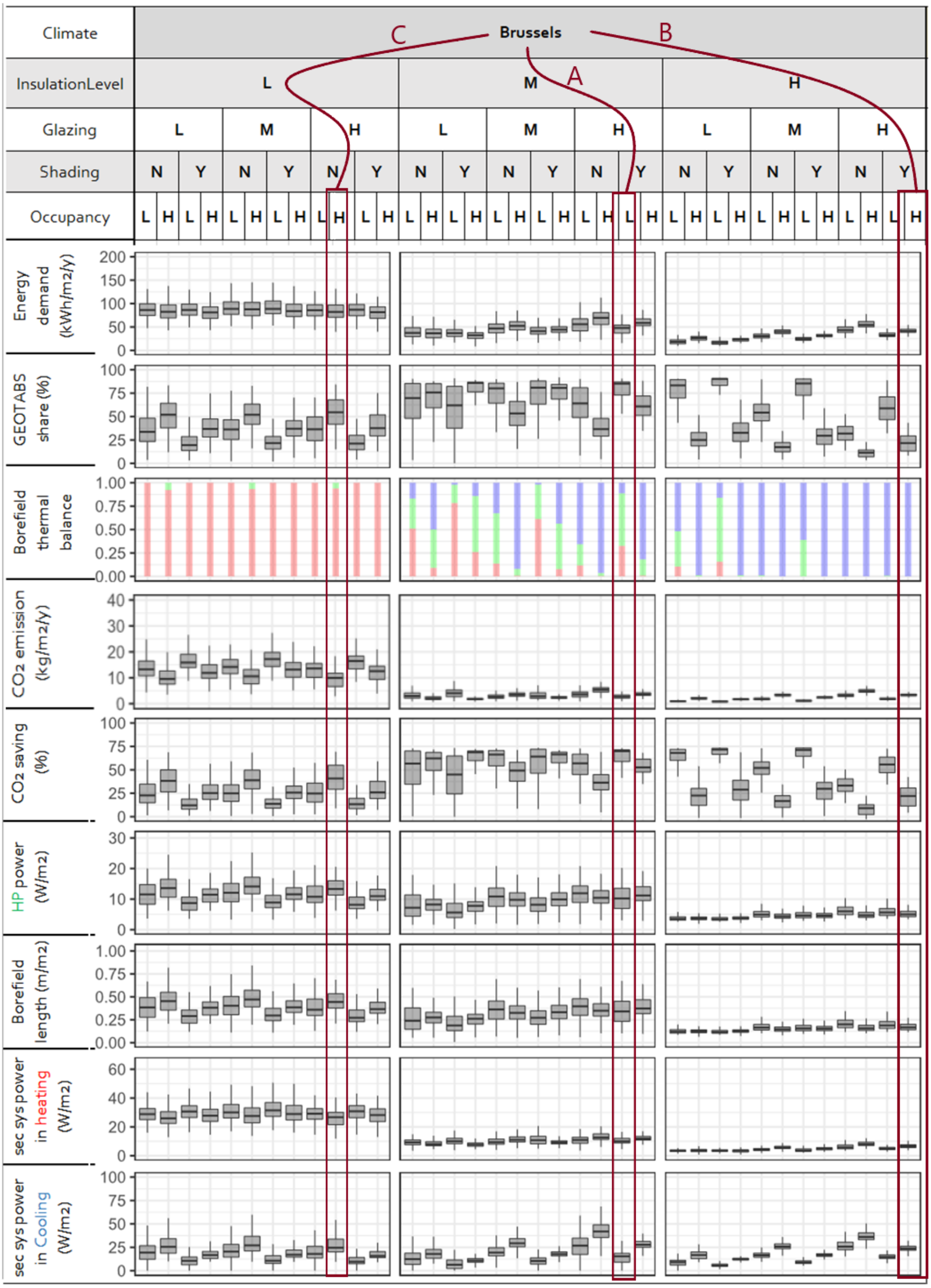


*Figure 5-4 Final decision tree for office typology in central European climate (Brussels)*

Figure 5-4 shows an excerpt of the final decision tree for the office typology. Note that in the decision tree, L"," M", and "H" respectively stand for "Low", "Medium" and "High" for different parameters. The meaning of "Low", "Medium", and "High" for different parameters, is explained in detail in D2.2 of the project [7]. A hands-on overview of these parameters is provided in *Annex 3: Building Parameters*. The complete trees are efficiently formatted for A3 size of paper and attached to this document in *Annex 4: Decision trees*. For each branch of the tree, the distribution of the following sizing and performance indicators is given:

- Energy demand (kWh/m².year): sum of net heating and cooling demands of the building assuming an ideal heating and cooling system (22-24°C indoor temperature range)
- GEOTABS share (%): share of the heating and cooling demands covered by GEOTABS (after the balancing assumption is applied)
- Borefield thermal balance: relative frequency of heating dominated, balanced (60%-40% rule) or cooling dominated (before the balancing assumption is applied) cases
- $CO_2$-emissions (kg$CO_2$/m².year): estimated $CO_2$-emissions for heating and cooling the building
- $CO_2$-savings (%): savings in $CO_2$-emissions as compared to a nonGEOTABS scenario (100% of heating and cooling provided by a boiler and chiller)
- HP-power (W/m²): specific power of the heat pump per conditioned floor area
- Borefield length (m/m²): length of the geothermal borefield (m) per conditioned floor area (m²)
- Sec Sys power in heating (W/m²): specific power of the secondary heating system per conditioned floor area
- Specific $Q_{design}$ in heating (W/m²): $Q_{design}$ (calculated according to *Annex 2: Qdesign calculation methodology*) per conditioned floor area
- Sec Sys power in cooling (W/m²): specific power of the secondary cooling system per conditioned floor area
- Specific $Q_{design}$ in heating (W/m²): $Q_{design}$ (calculated according to *Annex 2: Qdesign calculation methodology*) per conditioned floor area

Using the provided decision tree, we size the three case studies in Brussels (BrusselsA, BrusselsB, and BrusselsC as used in chapter 3). They are positioned in Figure 5-4 and the related design indicators values are derived accordingly. As the decision tree mostly provides the parameters vales per unit of conditioned floor area, the estimated values from the tree can be multiplied by the conditioned area (2390 m² for these cases) and the absolute values are derived. The estimated design indicators for the three case studies are listed in Table 5-1. Note that the values are rough approximations used in the early stage of the design procedure. We used the maximum value of the boxes in the box-plots (the 75% quartile of the distribution) for each indicator. The designer may decide to use the maximum value of the whiskers for a more conservative estimation. Moreover, it is possible to use more conservative scenario for one indicator, e.g the secondary system in heating and a less conservative scenario for the (usually more expensive) primary system.

*Table 5-1 Estimated values of design indicators for the three case studies in Brussels based on the proposed decision tree*

| Case | Total heat demand (kWh/m²/y) | GEOTABS share (%) | Heat pump power (kW) | Borefield length (m) | Secondary system power in heating (kW) | Secondary system power in cooling (kW) |
|---|---|---|---|---|---|---|
| **BrusselsA** | 55 | 87 | 31 | 950 | 24 | 43 |
| **BrusselsB** | 40 | 25 | 12 | 430 | 18 | 60 |
| **BrusselsC** | 90 | 65 | 35 | 1195 | 71 | 84 |

In comparison to the values reported in chapter 3 the accuracy is promising especially in comparison to the $Q_{design}$ as the traditional way of sizing HVAC components. This shows a remarkable downsizing of the components, while the sizing is still safe compared to the sizing derived from a detailed algorithm reported in section 3. Also, the rather limited power of the heat pump, when optimally controlled, allows to foresee a significant share of the heating and cooling demand. The GEOTABS share is approximated with the so-called "40-60 balancing rule" and accordingly results in a rather 'safe' and conservative estimation of the geothermal source. As noted in chapter 3, in a dedicated design of the borefield a higher imbalance between the heat injected and extracted from the field may be allowed without harming the long-term borefield performance, and thus to increase the share of GEOTABS. Moreover, use of RES for regeneration of the borefield (e.g. using a solar boiler or cooling tower) is also a design option that can be considered[5]. The thermal balance of borefield (second indicator) shows that BrusselsC is definitely heating dominated and BrusselsB is cooling dominated. BrusselsA seems the best design as the GEOTABS share is the highest and the $CO_2$ emission and saving is high.

The borefield length as the most important item in the investment costs, as observed in D2.4 [3], is approximated with a high accuracy and expectedly the investment cost is estimated with good accuracy.

## 5.3. Standardised modular key component packages

Note that the original objective of task 2.4 includes the selection of hybridGEOTABS modular component packages. The distributions of key components, such as those shown in chapter 4.2, provide the industrial partners with insights on the most frequently needed sizing ranges. Moreover, the decision trees provide insight in the relationship between the sizes of the various components, and can be used to create package solutions for the 'branches' of the trees. Therefore, this report provides the basis for the creation of key component packages.

At this point, based on an observation of the sizing distributions of the key components in chapter 4.2, the industrial partners concluded that the required powers in the building stock are all marketable and the sizes are very common sizes in the existing product families of manufacturers. Moreover, with the newly developed sizing guidelines, such as the decision trees presented in this work, that are very easy to apply and provide good insights in the relationships between component sizes for various groups of buildings, there is no need to fix or limit the sizing to fixed component packages, but rather the added value of this work is to provide case-specific optimal solutions based on commonly available components in the product ranges.

[5] Note that the design procedure and decision trees set out the performance of the GEOTABS concept (with borefield thermal balance) assuming a traditional secondary heating and cooling system (boiler and chiller). The results should therefore be interpreted as a minimum improvement in sustainability possible by the hybridGEOTABS concept. The designer is encouraged to use additional renewable sources in the secondary systems and/or provide the heat pump electricity from renewable sources, and further increase the environmental performance. D6.5 (and the project website) provide hydraulic schemes for such integrated hybridGEOTABS solutions, and the feasibility results of the design web-tool also provide a few renewable options (D2.6). Moreover, the hybridGEOTABS demonstration buildings (D4.1-2 and D4.11) provide fine real-life examples of the integration of additional renewable sources.

# 6. Conclusion

Starting from the EU building stock analysis, hourly dynamic heating and cooling loads of 140,000 case study buildings are simulated for one year in T2.2 (D2.2). The aforementioned dynamic thermal loads were made to be used for developing a fast and automated sizing methodology for hybridGEOTABS components. As a first important step, in T2.1 a load splitting algorithm called "baseload algorithm" was developed and validated. The load splitting algorithm receives the building load time series and splits the load between the primary and the secondary system optimally while maintaining thermal comfort and taking into account the dynamic thermal behaviour of TABS. The main outcomes of the load splitting algorithm are time series of the primary and the secondary system power for one year. The time series are then used in T2.4 for sizing the key components of hybridGEOTABS and estimating the environmental performance.

In this report, the steps and assumptions which are needed to go from the split time series to the final sizing and performance estimation were elaborated. First, the estimation of the geothermal heat pump size, based on smoothing of the baseload time series, is explained and validated. In a second post-processing step the thermal balance of the borefield was implemented based on the assumption that the heat injected to the borefield accounts for 40% to 60% of the total heat exchanged between the borefield and the building ("the 40-60 rule"). A complete overview of this calculation-efficient hybridGEOTABS sizing and performance estimation process is incorporated in section 2.6. The procedure is then applied to the 5 case-study buildings used in D2.4, and the outcomes are compared to the outcomes provided by a detailed, but more calculation-intensive, optimal sizing algorithm developed in T2.3 of the project. It is concluded that the results of the hybridGEOTABS sizing process are in the same order of magnitude, or a bit on the 'safe side' (higher), which is a welcome result in context of a pre-design study. In general, the outcomes of both design methods lead to a clearly smaller sizing than traditional steady-state design calculations. Secondly, the results indicate that the borefield balancing using the "40-60 rule" should be understood as "cautious" results, while higher imbalances between injected and extracted heat in the borefield may not harm the long-term performance of the borefield. Therefore, the results of the sizing process can be understood as a 'minimum' feasible share of GEOTABS, restricted by the thermal borefield balance, while from the perspective of the TABS only shares higher than 75% are feasible for the majority of building cases, representing the further optimisation potential in a more detailed borefield design and/or consideration of borefield regeneration options.

Finally, the hybridGEOTABS sizing and performance estimation process is applied to over 140,000 case-study buildings using an automated software code. The results provide a rich database as a basis for the hybridGEOTABS design webtool (D2.6). In the current report, meta-analysis of the data is carried out to come up with design guidelines for the key components of hybridGEOTABS. The main outcome of the whole procedure is a set of four design decision trees providing the most crucial inputs for the designer to consider in the early design stage, and the key sizing and performance indicators. The decision trees are provided for four different typologies attached to this report, and are available on the hybridGEOTABS website. While using the decision tree for design is very fast and easy, the results are close to the results coming from detailed and time consuming algorithms, and are thus an added value for the designer to assess the feasibility of hybridGEOTABS for their design. Moreover, architects can see the influence of different parameters on the sizing and performance of the system. Thus, they may use it to optimise the building physical design to increase the possible share of GEOTABS as a sustainable core for the building heating and cooling energy use.

*Note that the design procedure and decision trees set out the performance of the GEOTABS concept (with borefield thermal balance) assuming a traditional secondary heating and cooling system (boiler and chiller). The results should therefore be interpreted as a minimum improvement in sustainability possible by the hybridGEOTABS concept. The designer is encouraged to use additional renewable sources in the secondary systems and/or provide the heat pump electricity from renewable sources, and further increase the environmental performance. D6.5 (and the project* *website) provide hydraulic schemes for such integrated hybridGEOTABS solutions, and the feasibility results of the design web-tool also provide a few renewable options (D2.6). Moreover, the hybridGEOTABS demonstration buildings (D4.1-2 and D4.11) provide fine real-life examples of the integration of additional renewable sources.*

# Bibliography

1. Boydens, W., Helsen, L., Olesen, B.W., Ferkl, L., Laverge, J., & Himpe, E. (ed.). (2021a). Renewable and storage-integrated systems to supply comfort in buildings. A&S/books. Ghent (BE). Available from: www.hybridgeotabs.eu
2. Mahmoud, R., Himpe, E., Delghust, M., & Laverge, J. (2020). A modelling approach to reduce the simulation time of building stock models. In V. Corrado, E. Fabrizio, A. Gasparella, & F. Patuzzi (Eds.), Proceedings of Building Simulation 2019 : 16th Conference of IBPSA (Vol. 16, pp. 1491–1497). Rome, Italy: International Building Performance Association (IBPSA).
3. Sharifi, M., Jorissen, F. , Himpe, E., Helsen, L. & Laverge, J. (2020). Quantified differences in optimal TABS, HP and GSHX sizing for MPC and RBC. EU-H2020-hybridGEOTABS project Deliverable 2.4.
4. Sharifi, M., Mahmoud, R., Himpe, E., & Laverge, J. (2019a). Integrated sizing methodology for a hybridGEOTABS building. In ASHRAE TRANSACTIONS (Vol. 125, pp. 222–230). Kansas City, Kansas, USA.
5. Sharifi, M., Mahmoud, R., Himpe, E., & Laverge, J. (2019b). Interaction of GEOTABS and secondary heating and cooling systems in hybridGEOTABS buildings : towards a sizing methodology.
6. Sourbron, M., (2012). Dynamic thermal behaviour of buildings with concrete core activation. PhD thesis.
7. Mahmoud, R., Borrajo Bastero, J., Himpe, E. & Laverge, J. (2020). A set of parametric geometries for the (sub)typologies studied. EU-H2020-hybridGEOTABS project Deliverable 2.2.
8. Kavanaugh, S., Rafferty, K., (2014). Geothermal Heating and Cooling Design of Ground-Source Heat Pump Systems, book by ASHRAE.
9. https://cran.r-project.org/web/packages/partykit/partykit.pdf
10. Loh, Wei Yin. 2014. "Fifty Years of Classification and Regression Trees." International Statistical Review 82 (3): 329–48. https://doi.org/10.1111/insr.12016.

# List of Figures

# List of Tables

# Annex 1: Case-studies

**Geometrical form of the case study:**

We choose one office building typology with a fixed geometry, and we varied the building physical properties such as the climate, thermal insulation and air tightness level, orientation, shading type and internal heat gains, which results in 9 different cases. The geometrical properties of the selected case are summarized in the tables below. To generate the building geometrical form in order to be used as an input for modelling the building in the simulation tool Modelica, we applied a fitting process that is discussed in detail in D2.2.

| *Geometrical variables* | |
|---|---|
| ***Area [m²]*** | *2390* |
| ***Volume [m³]*** | *8532* |
| ***Heat loss surface area [m²]*** | *4325* |
| ***Height [m]*** | *6.4* |
| ***Number of floors*** | *2* |
| ***Window to wall ratio [%]*** | *38* |
| ***Compactness*** | *1.9* |

| ***Dimensions*** | |
|---|---|
| ***a [m]*** | ***15.5*** |
| ***n*** | ***2*** |
| ***h1 [m]*** | ***3.22*** |
| ***L [m]*** | ***57*** |
| ***B [m]*** | ***39*** |

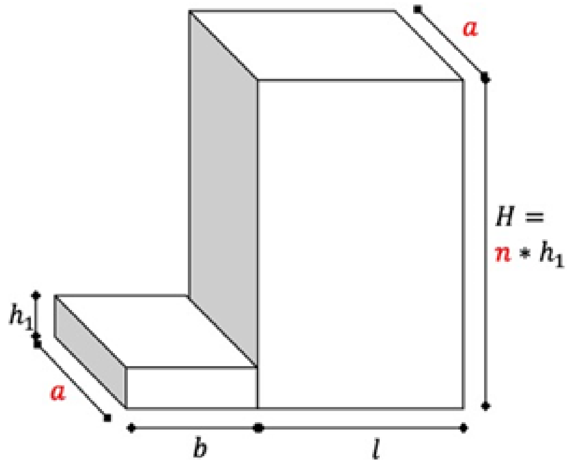


**Model description:**

We used a multi-zone modelling approach for modelling and simulation of the case study. The building model has 2 floors with a total of 11 zones: each floor has 5 zones, and there is an attached zone to the building volume as shown in . The building zones are divided based on typical office building functions such as: landscape offices, closed offices, a restaurant, meeting rooms and services zone as illustrated in the figure below.

**Building physical parameters:**

Five building physical properties were varied in this exercise.

(a) Climate: We used three weather files that can cover most of the EU-different climates such as Brussels (Maritime, temperate warm), Madrid (continental subtropical) and Warsaw (transitional, temperate warm).

(b) Thermal insulation and air tightness level: we used three levels of thermal insulation of the building envelope and windows as well as the air infiltration rate, summarized in. The three groups were decided based on the current regulations and codes for buildings in the different EU countries. Setting (1) represents a building with lower thermal transmission and high airtightness according to the passive house standards, setting (2) represents a building with average thermal transmission and airtightness according to today's energy performance regulations observed in many EU countries, and setting (3) represents a building that has higher thermal transmission and lower airtightness as observed in some Mediterranean regulations today and older buildings.

| | U-value opaque [W/m². K] | U-value windows [W/m². K] | Airtightness at n50 value 1/h |
|---|---|---|---|
| **High** | 0.15 | 0.80 | 0.6 |
| **Medium** | 0.27 | 1.5 | 2.0 |
| **Low** | 0.50 | 2.5 | 5.0 |

(c) Occupancy profiles: we identified two categories for internal heat gain profiles in offices based on the office density, such as low dense office and high dense office. The internal heat gains dynamic profiles account for occupancy, lighting and vary throughout the day and week. For the low dense office, the internal heat gains are on average 18 W/m², and for a high dense office on average 33 W/m².

(d) Shading system: We choose two options, either buildings with window shading system where an external screen is controlled for all windows. The external screen goes down (on) when solar irradiation on external windows exceeds 150 W/m². The second option is the use of no shading system.

(e) Orientation: We choose two orientations, west or south, where the largest facade is either facing the west or the south directions.

The 9 cases that were selected are summarized in the table below and are a reflection of the variety of cases in the building stock in T2.2. Note that not all these cases are equally likely to occur in practice. E.g. the low insulation group C is more likely to occur in the warmer regions of Europe in new buildings and using them in colder climates will cause a significant heat demand, for which low temperature emission systems such as TABS are less suited.

| Group | Climate | Thermal insulation group | Occupancy | Shading system | Orientation |
|---|---|---|---|---|---|
| [A] | Brussels | Medium | Low-dense | yes | North |
| | Madrid | Medium | Low-dense | yes | North |
| | Warsaw | Medium | Low-dense | yes | North |
| [B] | Brussels | High | High-dense | yes | North |
| | Madrid | High | High-dense | yes | North |
| | Warsaw | High | High-dense | yes | North |
| [C] | Brussels | Low | High-dense | No | West |
| | Madrid | Low | High-dense | No | West |
| | Warsaw | Low | High-dense | No | West |

**Heating and cooling demands of the case-studies**

In order to introduce the energy-related behaviour of the case-studies, the total yearly heating and cooling demands are presented, providing insight in the amounts of energy the building would require to maintain thermal comfort, to observe the balance between heating and cooling etc. To obtain the heating and cooling demands of the building, the building envelope model, explained in previous section, is coupled to an ideal heating and cooling system. The ideal heating and cooling system maintains the thermal comfort by giving/receiving energy to/from the building as much as needed to keep the temperature of different zones in the building between 22°C and 24°C. The hourly demand is calculated for all the year. Then, to have the load duration curves, the hourly demands are sorted from the maximum to the minimum value (zero). By that, the maximum value, the behaviour of the load, and the thermal (im)balance are recognised from the graph. The cooling demand is shown in negative numbers to be separated from the heating demand for increasing the readability of the graphs (see figure below).

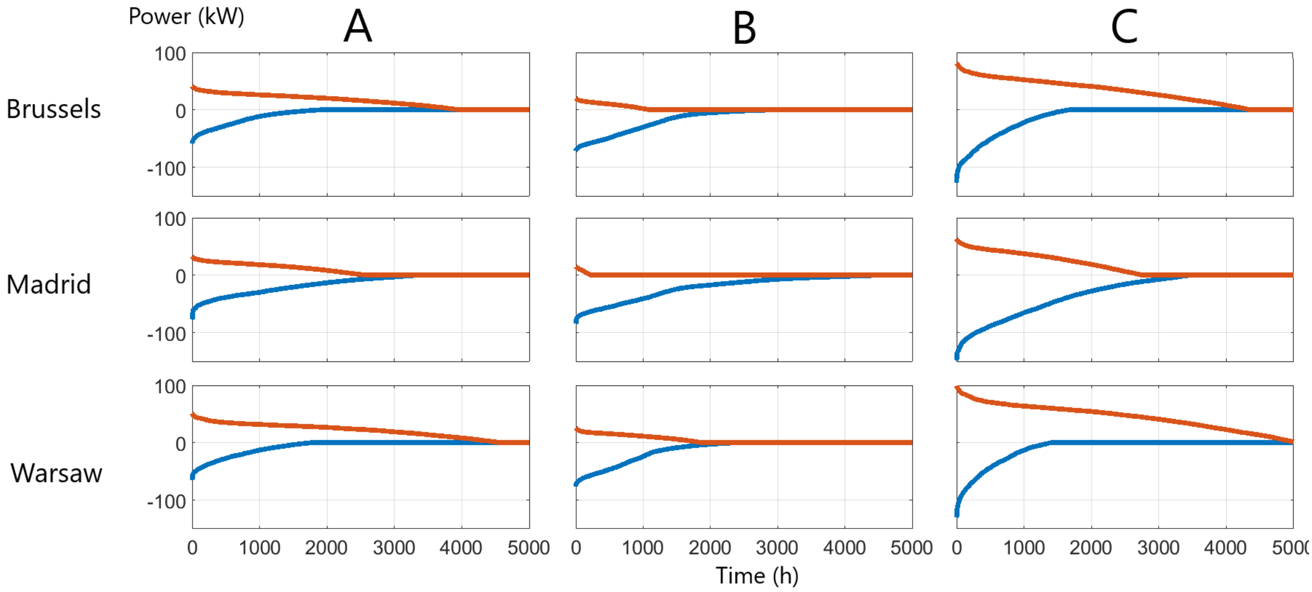


The highest energy use for heating and cooling is observed in the cases C, that are the cases with the lowest insulation and airtightness levels (see figure below). These buildings are very susceptible to climatic conditions (temperature, wind and solar gains) and to high internal gains. The cases A have a more typical or average insulation and air tightness level and a less dense occupation and shading, which will lead to considerably lower fluctuations in heating and cooling demands than in cases C. Logically, in Madrid, all cases C and A are cooling dominated, while in Brussels and Warsaw the cases are heating dominated. Finally, the cases B are highly insulated and shaded – similar to passive houses – but have a high dense occupation. This results on one hand in a very low heating demand (also in Brussels and Warsaw), but also in considerable cooling demands, to compensate for the high internal heat gains that are 'trapped' in the heavily insulated building.

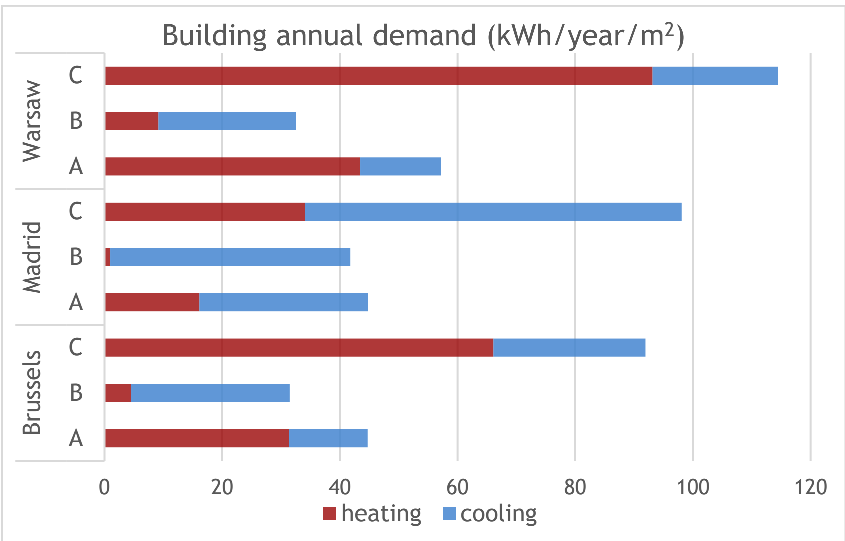

# Annex 2: $Q_{design}$ calculation methodology

To be able to compare the sizing with existing and traditional sizing approaches, the steady state heat loss and heat gains of the building are calculated. To be able to make a simple and fast methodology for estimation of the building maximum heating and cooling demand, different standards were investigated. Moreover, we had the dynamic simulation results for over 140,000 case studies which enabled us to test the proposed methodology for calculating the maximum steady state loads and compare it with dynamic simulation. The aim was to make sure that steady state $Q_{design}$ gives a safe value which is close to the standards as well. Therefore, some numbers were derived from the comparison between the results coming from the proposed methodology and the dynamic simulations. First, we briefly provide all the equations and assumptions needed for $Q_{design}$ calculation. Then, we show the comparison between $Q_{design}$ and the maximum thermal load of the building with dynamic simulations.

Maximum ***heating*** demand of the building based on steady state calculations for the worst case scenario as we assume solar and internal gains are zero:

$Q_{designHeating} = Q_{Inf} + Q_{ventilation} + Q_{RH} + Q_{Transmission}$

Where

$Q_{Infiltration}$ =1012*1.204*V/3600*n50/ $C_o$*(Tset - Tdes)

Where V is the volume of the building (m3)

$C_0$=20 "Conversion factor for n50 to Air Change Rate (annual average) Based EN ISO 13789

Qventilation = 1012*1.204 / 3600 * qvent * (1- efficiency) * (Tset – Tdes)

Where q is ventilation flow rate in $m^3$/h (= Volume ($m^3$) * air change rate (1/h))

Efficiency is heat recovery efficiency of ventilation system which is considered 85 % here

$Q_{RH}$=A*$f_{RH}$

A is the total conditioned area (m2)

For **residential** buildings $f_{RH}$=7

For **non-residential** buildings $f_{RH}$=11

Reheat factor based on EN 12831

$Q_{Traansmission} = (U_G * A_G + U_W*A_W+U_{roof}*A_{roof})*(T_{set} – T_{Out.Design.Heat})+ U_{GrFlroor}*A_{GrFlr}*( T_{set} – T_{Ground.Design})$

$U_{roof}$ and $U_{GrFloor}$ are the same as $U_W$ (U-value of the building walls)

Tset = 23;

The building parameters for different typologies are listed here in the following tables:

| Climate | $T_{out.design.Heat}$(˚C) | $T_{Ground.design}$(˚C) | $T_{out.design.Cool}$(˚C) |
|---|---|---|---|
| Brussels | -8 | 10 | 31 |
| Warsaw | -16 | 10 | 31 |
| Madrid | -3 | 12 | 35 |

| Schools | G-values of windows | U-values of walls | U-values of windows |
|---|---|---|---|
| Group A | 0.40 | 0.15 | 0.80 |
| Group B | 0.56 | 0.27 | 1.50 |
| Group C | 0.60 | 0.50 | 2.50 |

| Residentials | G-values of windows | U-values of walls | U-values of windows |
|---|---|---|---|
| Group A | 0.40 | 0.15 | 0.80 |
| Group B | 0.56 | 0.27 | 1.50 |
| Group C | 0.60 | 0.50 | 2.50 |

| Elderly Homes | G-values of windows | U-values of walls | U-values of windows |
|---|---|---|---|
| Group A | 0.40 | 0.15 | 0.80 |
| Group B | 0.56 | 0.27 | 1.50 |
| Group C | 0.60 | 0.50 | 2.50 |

| Office | G-values of windows | U-values of walls | U-values of windows |
|---|---|---|---|
| Group A | 0.40 | 0.15 | 0.80 |
| Group B | 0.56 | 0.27 | 1.50 |
| Group C | 0.60 | 0.50 | 2.50 |

Maximum ***cooling*** demand based on the worst case scenario:

$\mathbf{Q_{designCooling}} = Q_{Solarmax}+Q_{internalGainmax}+Q_{Transmission}+ Q_{Inf} + Q_{ventilation}$

Where

$Q_{Inf}$ and $Q_{ventilation}$ as explained for heating mode.

$\mathbf{Q_{Solarmax}} = I_{hor.max}$*Aw*Gw*ShadingCoeff

Gw is overall solar *Heat Gain Coefficient* of the window explained in ASHRAE fundamentals chapter 29, Table 11

This value is assumed for all the windows.

**ShadingCoeff**=0.5 if the building has shading system.

The number for *ShadingCoeff* is assumed based on the analysis that were carried out to find the best number that suits different cases.

$I_{hor.max}$ = maximum daily average of solar irradiation on a horizontal plane (W/m2)

Table below is used for maximum solar irradiations, values are for hottest summer scenario according to "meteonorm" program.

| Climate | Brussels | Warsaw | Madrid |
|---|---|---|---|
| Maximum daily average of solar irradiation(w/m2) | 365 | 367 | 396 |

$\mathbf{Q}_{\mathbf{internalGainMax}}$ is the maximum internal gains in W. the values Are reported in Annex 3.

$\mathbf{Q}_{\mathbf{Traansmission}} = (U_G*A_G + U_W*A_w+U_{roof}*A_{roof})*(T_{set} - T_{Out.Design.cooling})+ U_{GrFlr}*A_{GrFlr}*( T_{set} - T_{Ground.Design})$

As explained for heating mode. The only difference is the $T_{out.design}$.

As mentioned earlier, the maximum dynamic demand could be compared to the steady maximum steady state thermal load. Figure below shows such comparison for the office cases in heating mode. The ratio is chosen in such a way that the stability in its calculation is kept to have efficient visualisation. Therefore, the ratio is as follows

Ratio= (QdesignHeating-MaximumDynamicHeatingLoad)/ QdesignHeating

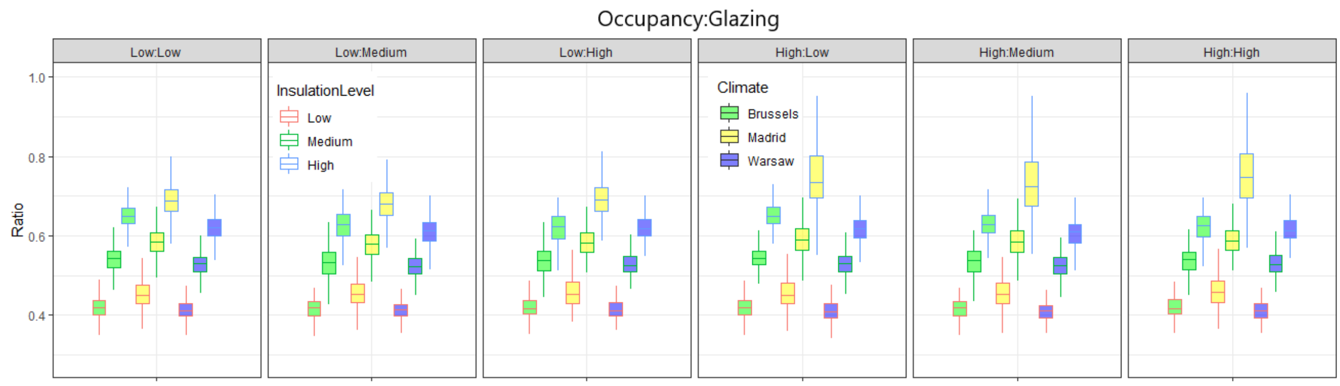


As seen in the figure, the overestimation of the maximum thermal load is observed. However, the overestimation is more pronounced in more insulated buildings. Nothing more than insulation level is effective on the overestimation as the figure shows. Glazing is perceived as an important factor specially in Madrid climate.

The figure shows the importance of using dynamic simulation specially for building which are high insulated (well suited) for sustainable HVAC systems. In other words, although expectedly using $Q_{design}$ ends up with overestimation of the required installed power for the conventional system, it is even worse when talking about sustainable approaches such as GEOTABS. Therefore, it is strongly recommended to have dedicated design methodologies for state-of-the-art HVAC solutions as the traditional design methods might even appear as a barrier against sustainable solutions. We provide the $Q_{design}$ since the as one of the indicators for each subgroup because the design should be able to compare the GEOTABS scenario with a non-GEOTABS scenario with conventional systems sized with traditional methodologies.

# Annex 3: Building parameters

A summary of the parameters used in the modelling and simulation of the four typologies. Those parameters are varied across the building geometries that are found in the EU building stock.

| | *Parameters* | | *Office building* | *School building* | *Elderly home* | *Multi-family* |
|---|---|---|---|---|---|---|
| **Window to wall ratio** | *Lower value* | | 20% | 20% | 20% | 20% |
| | *Average value* | | 40% | 40% | 35% | 35% |
| | *Upper value* | | 60% | 60% | 50% | 50% |
| **Orientation (large facade)** | *Lower value* | | South | South | South | South |
| | *Upper value* | | West | West | West | West |
| **Shading System** | *Lower value* | | No-Shading | No-Shading | No-Shading | No-Shading |
| | *Upper value* | | External screen is on at 150 (W/m$^2$) | External screen is on at 150 (W/m$^2$) | External screen is on at 150 (W/m$^2$) | External screen is on at 150 (W/m$^2$) |
| **Envelope performance** | *lower value* | Envelope U-value | 0.5 (w/m$^2$.k) | 0.5 (w/m$^2$.k) | 0.5 (w/m$^2$.k) | 0.5 (w/m$^2$.k) |
| | | Window U-value | 2.5(w/m$^2$.k) | 2.5(w/m$^2$.k) | 2.5(w/m$^2$.k) | 2.5(w/m$^2$.k) |
| | | Glass g-value | 0.6 | 0.6 | 0.6 | 0.6 |
| | | air-tightness n50 | 5.0 (h$^{-1}$) | 5.0 (h$^{-1}$) | 5.0 (h$^{-1}$) | 5.0 (h$^{-1}$) |
| | *Average value* | Envelope U-value | 0.27 (w/m$^2$.k) | 0.27 (w/m$^2$.k) | 0.27 (w/m$^2$.k) | 0.27 (w/m$^2$.k) |
| | | Window U-value | 1.5 (w/m$^2$.k) | 1.5 (w/m$^2$.k) | 1.5 (w/m$^2$.k) | 1.5 (w/m$^2$.k) |
| | | Glass g-value | 0.56 | 0.56 | 0.56 | 0.56 |
| | | air-tightness n50 | 2.0 ( h$^{-1}$) | 2.0 ( h$^{-1}$) | 2.0 ( h$^{-1}$) | 2.0 ( h$^{-1}$) |
| | *Upper value* | Envelope U-value | 0.15 (w/m$^2$.k) | 0.15 (w/m$^2$.k) | 0.15 (w/m$^2$.k) | 0.15 (w/m$^2$.k) |
| | | Window U-value | 0.8 (w/m$^2$.k) | 0.8 (w/m$^2$.k) | 0.8 (w/m$^2$.k) | 0.8 (w/m$^2$.k) |

| | | | | | | |
|---|---|---|---|---|---|---|
| | | Glass g-value | 0.4 | 0.4 | 0.4 | 0.4 |
| | | air-tightness n50 | 0.6 ( h$^{-1}$) | 0.6 ( h$^{-1}$) | 0.6 ( h$^{-1}$) | 0.6 ( h-1) |
| **Building mass** | Lower value | | 390 (kg/m$^2$) | 391 (kg/m$^2$) | 392 (kg/m$^2$) | 207 (kg/m$^2$) |
| | Upper value | | 630 (kg/m$^2$) | 630 (kg/m$^2$) | 630 (kg/m$^2$) | 661 (kg/m$^2$) |
| **Internal heat gains** | | | **Office zone** | **Classroom zone** | **Elderly room zone** | **Apartments zone** |
| | *Lower value* | Density | 1Person/20m$^2$ | 1Student/3.5m$^2$ | ___ | 1 person / dwelling |
| | | *Occupancy* | 5.0 (W/m$^2$) | 21.0 (W/m$^2$) | 0 | 1.2 (W/m$^2$) |
| | | *Lighting* | 8.0 (W/m$^2$) | 8.0 (W/m$^2$) | 0 | 1.5 (W/m$^2$) |
| | | *Appliances* | 5.5 (W/m$^2$) | 4.0 (W/m$^2$) | 0 | 4.8 (W/m$^2$) |
| | | *Total* | 18.5 (W/m$^2$) | 33.0 (W/m$^2$) | 0 | 7.5 (W/m$^2$) |
| | *Upper value* | *Density* | 1Person/10m$^2$ | 1Student/2.5m$^2$ | 1Elderly/24m$^2$ | 3 people / dwelling |
| | | *Occupancy* | 10.0 (W/m$^2$) | 30.0 (W/m$^2$) | 3.0 (W/m$^2$) | 3.6 (W/m$^2$) |
| | | *Lighting* | 8.0 (W/m$^2$) | 8.0 (W/m$^2$) | 3.75 (W/m$^2$) | 2.0 (W/m$^2$) |
| | | *Appliances* | 15.0 (W/m$^2$) | 4.0 (W/m$^2$) | 4.0 (W/m$^2$) | 23.0 (W/m$^2$) |
| | | *Total* | 33.0 (W/m$^2$) | 42.0 (W/m$^2$) | 10.7 (W/m$^2$) | 28.6 (W/m$^2$) |
| **Ventilation flow rate** | *Constant* | | 36 (m$^3$/h) | 36 (m$^3$/h) | 50 (m$^3$/h) | 1 (m$^3$/m$^2$/h) dwellings 0.2 (m$^3$/m$^2$/h) staricases |
| **Operative temperature** | *Constant* | | 24 (°C) | 23 (°C) | 24 (°C) | 23 (°C) |

## Annex 4: Decision trees


Notes: 1- The borefield balance graph shows the relative frequency of cases which are inherently heating (red) or cooling (blue) dominated or balanced (green) in each subgroup.

2- "L"," M", and "H" respectively stand for "Low", "Medium",and "High" for different parameters. To know what "Low", "Medium", and "High" refers to for different parameters, read D2.2 of hybridGEOTABS project (available on www.hybridGEOTABS.eu)


Notes: 1- The borefield balance graph shows the relative frequency of cases which are inherently heating (red) or cooling (blue) dominated or balanced (green) in each subgroup.

2- "L"," M", and "H" respectively stand for "Low", "Medium",and "High" for different parameters. To know what "Low", "Medium", and "High" refers to for different parameters, read D2.2 of hybridGEOTABS project (available on www.hybridGEOTABS.eu)


Notes: 1- The borefield balance graph shows the relative frequency of cases which are inherently heating (red) or cooling (blue) dominated or balanced (green) in each subgroup.

2- In the elderly home typology, no differentiation is made between low and high occupancy levels (only one typical level is assumed)

3- "L"," M", and "H" respectively stand for "Low", "Medium",and "High" for different parameters. To know what "Low", "Medium", and "High" refers to for different parameters, read D2.2 of hybridGEOTABS project (available on www.hybridGEOTABS.eu)


Notes: 1- The borefield balance graph shows the relative frequency of cases which are inherently heating (red) or cooling (blue) dominated or balanced (green) in each subgroup.